

Probabilistic Line Searches for Stochastic Optimization

Maren Mahsereci

Philipp Hennig

Max Planck Institute for Intelligent Systems
Spemannstraße, 72076 Tübingen, Germany

MMAHSERECI@TUE.MPG.DE

PHENNIG@TUE.MPG.DE

Abstract

In deterministic optimization, line searches are a standard tool ensuring stability and efficiency. Where only stochastic gradients are available, no direct equivalent has so far been formulated, because uncertain gradients do not allow for a strict sequence of decisions collapsing the search space. We construct a probabilistic line search by combining the structure of existing deterministic methods with notions from Bayesian optimization. Our method retains a Gaussian process surrogate of the univariate optimization objective, and uses a probabilistic belief over the Wolfe conditions to monitor the descent. The algorithm has very low computational cost, and no user-controlled parameters. Experiments show that it effectively removes the need to define a learning rate for stochastic gradient descent.

Keywords: stochastic optimization, learning rates, line searches, Gaussian processes, Bayesian optimization

1. Introduction

This work substantially extends the work of Mahsereci and Hennig (2015) published at NIPS 2015. Stochastic gradient descent (SGD, Robbins and Monro, 1951) is currently the standard in machine learning for the optimization of highly multivariate functions if their gradient is corrupted by noise. This includes the online or mini-batch training of neural networks, logistic regression (Zhang, 2004; Bottou, 2010) and variational models (e.g. Hoffman et al., 2013; Hensman et al., 2012; Broderick et al., 2013). In all these cases, noisy gradients arise because an exchangeable loss-function $\mathcal{L}(x)$ of the optimization parameters $x \in \mathbb{R}^D$, across a large dataset $\{d_i\}_{i=1, \dots, M}$, is evaluated only on a subset $\{d_j\}_{j=1, \dots, m}$:

$$\mathcal{L}(x) := \frac{1}{M} \sum_{i=1}^M \ell(x, d_i) \approx \frac{1}{m} \sum_{j=1}^m \ell(x, d_j) =: \hat{\mathcal{L}}(x) \quad m \ll M. \quad (1)$$

If the indices j are i.i.d. draws from $[1, M]$, by the Central Limit Theorem, the error $\hat{\mathcal{L}}(x) - \mathcal{L}(x)$ is unbiased and approximately normal distributed. Despite its popularity and its low cost per step, SGD has well-known deficiencies that can make it inefficient, or at least tedious to use in practice. Two main issues are that, first, the gradient itself, even without noise, is not the optimal search *direction*; and second, SGD requires a *step size* (learning rate) that has drastic effect on the algorithm’s efficiency, is often difficult to choose well, and virtually never optimal for each individual descent step. The former issue, adapting the search direction, has been addressed by many authors (see George and Powell, 2006, for an overview). Existing approaches range from lightweight ‘diagonal preconditioning’ approaches

like ADAM (Kingma and Ba, 2014), ADAGRAD (Duchi et al., 2011), and ‘stochastic meta-descent’ (Schraudolph, 1999), to empirical estimates for the natural gradient (Amari et al., 2000) or the Newton direction (Roux and Fitzgibbon, 2010), to problem-specific algorithms (Rajesh et al., 2013), and more elaborate estimates of the Newton direction (Hennig, 2013). Most of these algorithms also include an auxiliary adaptive effect on the learning rate. And Schaul et al. (2013) recently provided an estimation method to explicitly adapt the learning rate from one gradient descent step to another. None of these algorithms change the size of the *current* descent step. Accumulating statistics across steps in this fashion requires some conservatism: If the step size is initially too large, or grows too fast, SGD can become unstable and ‘explode’, because individual steps are not checked for robustness at the time they are taken.

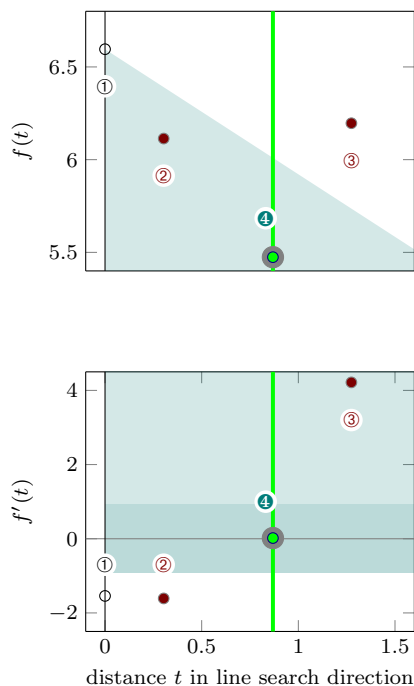


Figure 1: Sketch: The task of a *classic line search* is to tune the step taken by a optimization algorithm along a univariate search direction. The search starts at the endpoint ① of the previous line search, at $t = 0$. The *upper* plot shows function values, the *lower* plot corresponding gradients. A sequence of extrapolation steps ②, ③ finds a point of positive gradient at ③. It is followed by interpolation steps until an acceptable point ④ is found. Points of insufficient decrease, above the line $f(0) + c_1 t f'(0)$ (white area in upper plot) are excluded by the Armijo condition W-I, while points of steep negative gradient (white area in lower plot) are excluded by the curvature condition W-II (the strong extension of the Wolfe conditions also excludes the light green area in the lower plot). Point ④ is the first to fulfil both conditions, and is thus accepted.

The in principal same problem exists in deterministic (noise-free) optimization problems. There, providing stability is one of several tasks of the *line search* subroutine. It is a standard constituent of algorithms like the classic nonlinear conjugate gradient (Fletcher and Reeves, 1964) and BFGS (Broyden, 1969; Fletcher, 1970; Goldfarb, 1970; Shanno, 1970) methods (Nocedal and Wright, 1999, §3).¹ In the noise-free case, line searches are considered a solved problem (Nocedal and Wright, 1999, §3). But the methods used in deterministic optimization are not stable to noise. They are easily fooled by even small disturbances, either becoming overly conservative or failing altogether. The reason for this brittleness is that existing line searches take a sequence of hard decisions to shrink or shift the search

1. In these algorithms, another task of the line search is to guarantee certain properties of the surrounding estimation rule. In BFGS, e.g., it ensures positive definiteness of the estimate. This aspect will not feature here.

space. This yields efficiency, but breaks hard in the presence of noise. Section 3 constructs a probabilistic line search for noisy objectives, stabilizing optimization methods like the works cited above. As line searches only change the length, not the direction of a step, they could be used in combination with the algorithms adapting SGD’s direction, cited above. The algorithm presented below is thus a complement, not a competitor, to these methods.

2. Connections

2.1 Deterministic Line Searches

There is a host of existing line search variants (Nocedal and Wright, 1999, §3). In essence, though, these methods explore a univariate domain ‘to the right’ of a starting point, until an ‘acceptable’ point is reached (Figure 1). More precisely, consider the problem of minimizing $\mathcal{L}(x) : \mathbb{R}^D \rightarrow \mathbb{R}$, with access to $\nabla \mathcal{L}(x) : \mathbb{R}^D \rightarrow \mathbb{R}^D$. At iteration i , some ‘outer loop’ chooses, at location x_i , a search direction $s_i \in \mathbb{R}^D$ (e.g. by the BFGS rule, or simply $s_i = -\nabla \mathcal{L}(x_i)$ for gradient descent). It will *not* be assumed that s_i has unit norm. The line search operates along the univariate domain $x(t) = x_i + ts_i$ for $t \in \mathbb{R}_+$. Along this direction it collects scalar function values and projected gradients that will be denoted $f(t) = \mathcal{L}(x(t))$ and $f'(t) = s_i^\top \nabla \mathcal{L}(x(t)) \in \mathbb{R}$. Most line searches involve an initial extrapolation phase to find a point t_r with $f'(t_r) > 0$. This is followed by a search in $[0, t_r]$, by interval nesting or by interpolation of the collected function and gradient values, e.g. with cubic splines.²

2.1.1 THE WOLFE CONDITIONS FOR TERMINATION

As the line search is only an auxiliary step within a larger iteration, it need not find an exact root of f' ; it suffices to find a point ‘sufficiently’ close to a minimum. The *Wolfe conditions* (Wolfe, 1969) are a widely accepted formalization of this notion; they consider t acceptable if it fulfills

$$f(t) \leq f(0) + c_1 t f'(0) \quad (\text{W-I}) \quad \text{and} \quad f'(t) \geq c_2 f'(0) \quad (\text{W-II}), \quad (2)$$

using two constants $0 \leq c_1 < c_2 \leq 1$ chosen by the designer of the line search, not the user. W-I is the *Armijo* or *sufficient decrease* condition (Armijo, 1966). It encodes that acceptable functions values should lie below a linear extrapolation line of slope $c_1 f'(0)$. W-II is the *curvature condition*, demanding a decrease in slope. The choice $c_1 = 0$ accepts any value below $f(0)$, while $c_1 = 1$ rejects all points for convex functions. For the curvature condition, $c_2 = 0$ only accepts points with $f'(t) \geq 0$; while $c_2 = 1$ accepts any point of greater slope than $f'(0)$. W-I and W-II are known as the *weak* form of the Wolfe conditions. The *strong* form replaces W-II with $|f'(t)| \leq c_2 |f'(0)|$ (W-IIa). This guards against accepting points of low function value but large positive gradient. Figure 1 shows a conceptual sketch illustrating the typical process of a line search, and the weak and strong Wolfe conditions. The exposition in §3.3 will initially focus on the weak conditions, which can be precisely modeled probabilistically. Section 3.3.1 then adds an approximate treatment of the strong form.

2. This is the strategy in `minimize.m` by C. Rasmussen, which provided a model for our implementation. At the time of writing, it can be found at <http://learning.eng.cam.ac.uk/car1/code/minimize/minimize.m>

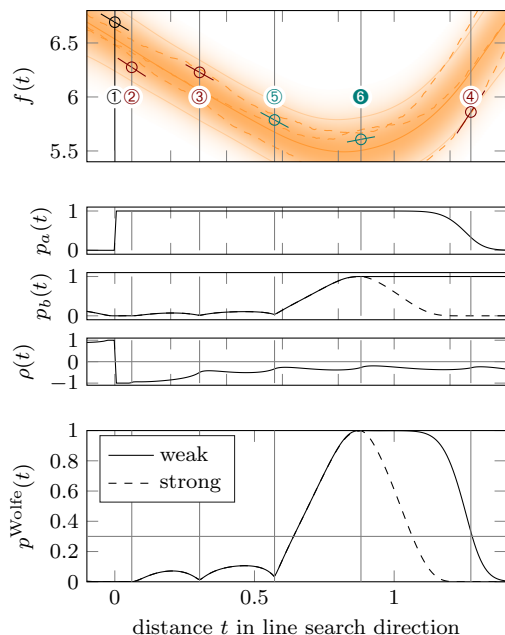


Figure 2: Sketch of a *probabilistic line search*. As in Fig. 1, the algorithm performs extrapolation (②,③,④) and interpolation (⑤,⑥), but receives unreliable, noisy function and gradient values. These are used to construct a GP posterior (top: solid posterior mean, thin lines at 2 standard deviations, local pdf marginal as shading, three dashed sample paths). This implies a bivariate Gaussian belief (§3.3) over the validity of the weak Wolfe conditions (middle three plots. $p_a(t)$ is the marginal for W-I, $p_b(t)$ for W-II, $\rho(t)$ their correlation). Points are considered acceptable if their joint probability $p^{\text{Wolfe}}(t)$ (bottom) is above a threshold (gray). An approximation (§3.3.1) to the strong Wolfe conditions is shown dashed.

2.2 Bayesian Optimization

A recently blossoming sample-efficient approach to global optimization revolves around modeling the objective f with a probability measure $p(f)$; usually a Gaussian process (GP). Searching for extrema, evaluation points are then chosen by a utility functional $u[p(f)]$. Our line search borrows the idea of a Gaussian process surrogate, and a popular utility, *expected improvement* (Jones et al., 1998). Bayesian optimization methods are often computationally expensive, thus ill-suited for a cost-sensitive task like a line search. But since line searches are governors more than information extractors, the kind of sample-efficiency expected of a Bayesian optimizer is not needed. The following sections develop a lightweight algorithm which adds only minor computational overhead to stochastic optimization.

3. A Probabilistic Line Search

We now consider minimizing $y(t) = \hat{\mathcal{L}}(x(t))$ from Eq. 1. That is, the algorithm can access only noisy function values and gradients y_t, y'_t at location t , with Gaussian likelihood

$$p(y_t, y'_t | f) = \mathcal{N} \left(\begin{bmatrix} y_t \\ y'_t \end{bmatrix}; \begin{bmatrix} f(t) \\ f'(t) \end{bmatrix}, \begin{bmatrix} \sigma_f^2 & 0 \\ 0 & \sigma_{f'}^2 \end{bmatrix} \right). \quad (3)$$

The Gaussian form is supported by the Central Limit argument at Eq. 1, see §3.4 regarding estimation of the variances $\sigma_f^2, \sigma_{f'}^2$. Our algorithm has three main ingredients: A robust yet lightweight Gaussian process surrogate on $f(t)$ facilitating analytic optimization; a simple Bayesian optimization objective for exploration; and a probabilistic formulation of the Wolfe conditions as a termination criterion. While Appendix D contains a detailed pseudocode,

Algorithm 1 PROBLINESEARCHSKETCH($f, y_0, y'_0, \sigma_{f_0}, \sigma_{f'_0}$)

$GP \leftarrow \text{INITGP}(y_0, y'_0, \sigma_{f_0}, \sigma_{f'_0})$
 $T, Y, Y' \leftarrow \text{INITSTORAGE}(t_0, y_0, y'_0)$ ▷ for observed points
 $t \leftarrow 1$ ▷ position of initial candidate

while budget not used and no Wolfe point found **do**

$[y, y'] \leftarrow f(x(t))$ ▷ evaluate objective
 $T, Y, Y' \leftarrow \text{UPDATESTORAGE}(t, y, y')$
 $GP \leftarrow \text{UPDATEGP}(t, y, y')$
 $P^{\text{Wolfe}} \leftarrow \text{PROBWOLFE}(T, GP)$ ▷ compute Wolfe probability at points in T

if any P^{Wolfe} above Wolfe threshold c_W **then**

return Wolfe point
else

$T_{\text{cand}} \leftarrow \text{COMPUTECANDIDATES}(GP)$ ▷ positions of new candidates
 $EI \leftarrow \text{EXPECTEDIMPROVEMENT}(T_{\text{cand}}, GP)$
 $PW \leftarrow \text{PROBWOLFE}(T_{\text{cand}}, GP)$
 $t \leftarrow$ where $(PW \odot EI)$ is maximal ▷ find best candidate in T_{cand}

end if

end while

return observed point in T with lowest GP mean since no Wolfe point found

Algorithm 1 very roughly sketches the structure of the probabilistic line search and highlights its essential ingredients.

3.1 Lightweight Gaussian Process Surrogate

We model information about the objective in a probability measure $p(f)$. There are two requirements on such a measure: First, it must be robust to irregularity of the objective. And second, it must allow analytic computation of discrete candidate points for evaluation, because a line search should not call yet another optimization subroutine itself. Both requirements are fulfilled by a once-integrated Wiener process, i.e. a zero-mean Gaussian process prior $p(f) = \mathcal{GP}(f; 0, k)$ with covariance function

$$k(t, t') = \theta^2 [1/3 \min^3(\tilde{t}, \tilde{t}') + 1/2 |t - t'| \min^2(\tilde{t}, \tilde{t}')]. \quad (4)$$

Here $\tilde{t} := t + \tau$ and $\tilde{t}' := t' + \tau$ denote a shift by a constant $\tau > 0$. This ensures this kernel is positive semi-definite, the precise value τ is irrelevant as the algorithm only considers positive values of t (our implementation uses $\tau = 10$). See §3.4 regarding the scale θ^2 . With the likelihood of Eq. 3, this prior gives rise to a GP posterior whose mean function is a cubic spline³ (Wahba, 1990). We note in passing that regression on f and f' from N observations

3. Eq. 4 can be generalized to the ‘natural spline’, removing the need for the constant τ (Rasmussen and Williams, 2006, §6.3.1). However, this notion is ill-defined in the case of a single observation, which is crucial for the line search.

of pairs (y_t, y'_t) can be formulated as a filter (Särkkä, 2013) and thus performed in $\mathcal{O}(N)$ time. However, since a line search typically collects < 10 data points, generic GP inference, using a Gram matrix, has virtually the same, low cost.

Because Gaussian measures are closed under linear maps (Papoulis, 1991, §10), Eq. 4 implies a Wiener process (linear spline) model on f' :

$$p(f; f') = \mathcal{GP} \left(\begin{bmatrix} f \\ f' \end{bmatrix}; \begin{bmatrix} 0 \\ 0 \end{bmatrix}, \begin{bmatrix} k & k^\partial \\ \partial k & \partial k^\partial \end{bmatrix} \right), \quad (5)$$

with (using the indicator function $\mathbb{I}(x) = 1$ if x , else 0)

$$\begin{aligned} k^\partial_{tt'} &:= \frac{\partial k(t, t')}{\partial t'} = \theta^2 [\mathbb{I}(t < t')t^2/2 + \mathbb{I}(t \geq t')(tt' - t'^2/2)] \\ \partial k_{tt'} &:= \frac{\partial k(t, t')}{\partial t} = \theta^2 [\mathbb{I}(t' < t)t'^2/2 + \mathbb{I}(t' \geq t)(tt' - t^2/2)] \\ \partial k^\partial_{tt'} &:= \frac{\partial^2 k(t, t')}{\partial t' \partial t} = \theta^2 \min(t, t') \end{aligned} \quad (6)$$

Given a set of evaluations $(\mathbf{t}, \mathbf{y}, \mathbf{y}')$ (vectors, with elements t_i, y_{t_i}, y'_{t_i}) with independent likelihood (3), the posterior $p(f | \mathbf{y}, \mathbf{y}')$ is a GP with posterior mean μ and covariance and \tilde{k} as follows:

$$\begin{aligned} \begin{bmatrix} \mu(t) \\ \mu'(t) \end{bmatrix} &= \underbrace{\begin{bmatrix} k_{tt} & k^\partial_{tt} \\ \partial k_{tt} & \partial k^\partial_{tt} \end{bmatrix} \begin{bmatrix} k_{tt} + \sigma_f^2 \mathbf{I} & k^\partial_{tt} \\ \partial k_{tt} & \partial k^\partial_{tt} + \sigma_{f'}^2 \mathbf{I} \end{bmatrix}^{-1}}_{=: \mathbf{g}^\top(t)} \begin{bmatrix} \mathbf{y} \\ \mathbf{y}' \end{bmatrix} \\ \begin{bmatrix} \tilde{k}(t, t') & \tilde{k}^\partial(t, t') \\ \tilde{\partial k}(t', t) & \tilde{\partial k}^\partial(t, t') \end{bmatrix} &= \begin{bmatrix} k_{tt'} & k^\partial_{tt'} \\ \partial k_{t't} & \partial k^\partial_{t't} \end{bmatrix} - \mathbf{g}^\top(t) \begin{bmatrix} k_{tt'} & k^\partial_{tt'} \\ \partial k_{t't} & \partial k^\partial_{t't} \end{bmatrix} \end{aligned} \quad (7)$$

The posterior marginal variance will be denoted by $\mathbb{V}(t) = \tilde{k}(t, t)$. To see that μ is indeed piecewise cubic (i.e. a cubic spline), we note that it has at most three non-vanishing derivatives⁴, because

$$\begin{aligned} \partial^2 k_{tt'} &:= \frac{\partial^2 k(t, t')}{\partial t^2} = \theta^2 \mathbb{I}(t \leq t') \\ \partial^3 k_{tt'} &:= \frac{\partial^3 k(t, t')}{\partial t^3} = \theta^2 \mathbb{I}(t \leq t')(t' - t) \\ \partial^2 k^\partial_{tt'} &:= \frac{\partial^4 k(t, t')}{\partial t^2 \partial t'} = -\theta^2 \mathbb{I}(t \leq t') \\ \partial^3 k^\partial_{tt'} &:= \frac{\partial^4 k(t, t')}{\partial t^3 \partial t'} = 0. \end{aligned} \quad (8)$$

This piecewise cubic form of μ is crucial for our purposes: having collected N values of f and f' , respectively, all local minima of μ can be found analytically in $\mathcal{O}(N)$ time in a single

4. There is no well-defined probabilistic belief over f'' and higher derivatives—sample paths of the Wiener process are almost surely non-differentiable almost everywhere (Adler, 1981, §2.2). But $\mu(t)$ is always a member of the reproducing kernel Hilbert space induced by k , thus piecewise cubic (Rasmussen and Williams, 2006, §6.1).

sweep through the ‘cells’ $t_{i-1} < t < t_i$, $i = 1, \dots, N$ (here $t_0 = 0$ denotes the start location, where (y_0, y'_0) are ‘inherited’ from the preceding line search. For typical line searches $N < 10$, c.f. §4). In each cell, $\mu(t)$ is a cubic polynomial with at most one minimum in the cell, found by a trivial quadratic computation from the three scalars $\mu'(t_i), \mu''(t_i), \mu'''(t_i)$. This is in contrast to other GP regression models—for example the one arising from a Gaussian kernel—which give more involved posterior means whose local minima can be found only approximately. Another advantage of the cubic spline interpolant is that it does not assume the existence of higher derivatives (in contrast to the Gaussian kernel, for example), and thus reacts robustly to irregularities in the objective.

In our algorithm, after each evaluation of (y_N, y'_N) , we use this property to compute a short list of *candidates* for the next evaluation, consisting of the $\leq N$ local minimizers of $\mu(t)$ and one additional *extrapolation* node at $t_{\max} + \alpha$, where t_{\max} is the currently largest evaluated t , and α is an extrapolation step size starting at $\alpha = 1$ and doubled after each extrapolation step.

3.2 Choosing Among Candidates

The previous section described the construction of $< N + 1$ discrete candidate points for the next evaluation. To decide at which of the candidate points to actually call f and f' , we make use of a popular utility from Bayesian optimization. *Expected improvement* (Jones et al., 1998) is the expected amount, under the GP surrogate, by which the function $f(t)$ might be smaller than a ‘current best’ value η (we set $\eta = \min_{i=0, \dots, N} \{\mu(t_i)\}$, where t_i are observed locations),

$$\begin{aligned} u_{\text{EI}}(t) &= \mathbb{E}_{p(f_t | \mathbf{y}, \mathbf{y}')} [\min\{0, \eta - f(t)\}] \\ &= \frac{\eta - \mu(t)}{2} \left(1 + \operatorname{erf} \frac{\eta - \mu(t)}{\sqrt{2\mathbb{V}(t)}} \right) + \sqrt{\frac{\mathbb{V}(t)}{2\pi}} \exp \left(-\frac{(\eta - \mu(t))^2}{2\mathbb{V}(t)} \right). \end{aligned} \quad (9)$$

The next evaluation point is chosen as the candidate maximizing this utility, multiplied by the probability for the Wolfe conditions to be fulfilled, which is derived in the following section. An illustration of the candidate proposal and selection is shown in Figure 3.

3.3 Probabilistic Wolfe Conditions for Termination

The key observation for a probabilistic extension of the Wolfe conditions W-I and W-II is that they are positivity constraints on two variables a_t, b_t that are both linear projections of the (jointly Gaussian) variables f and f' :

$$\begin{bmatrix} a_t \\ b_t \end{bmatrix} = \begin{bmatrix} 1 & c_1 t & -1 & 0 \\ 0 & -c_2 & 0 & 1 \end{bmatrix} \begin{bmatrix} f(0) \\ f'(0) \\ f(t) \\ f'(t) \end{bmatrix} \geq 0. \quad (10)$$

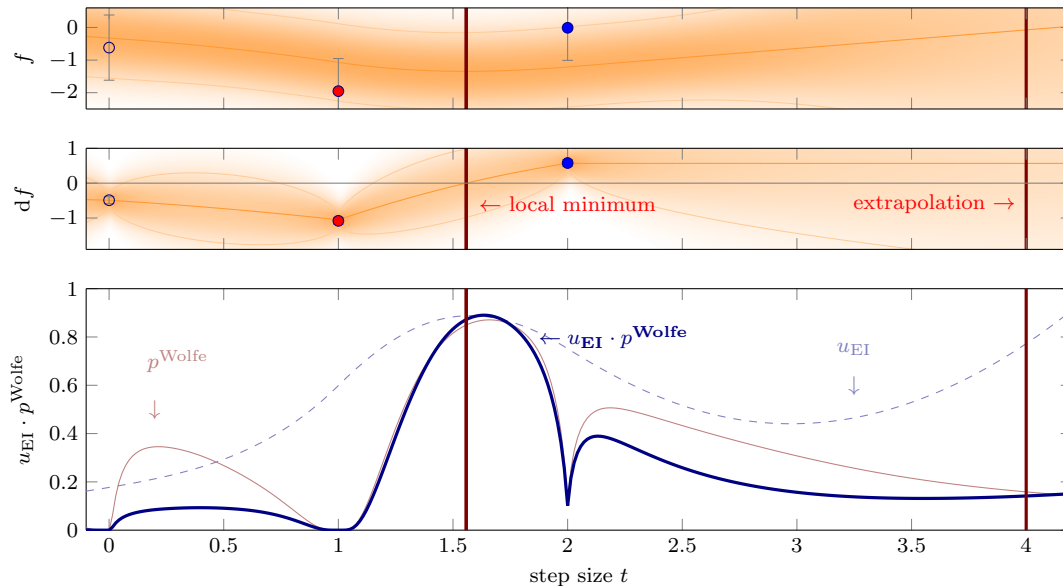


Figure 3: Illustration of *candidate selection* by Bayesian optimization. Top: GP marginal posterior of function values. Posterior mean in solid orange and, two standard deviations in thinner solid orange, local pdf marginal as shading. The red and the blue point are evaluations of the objective function, collected by the line search. Middle: GP marginal posterior of corresponding gradients. Colors same as in top plot. In all three plots the locations of the *two* candidate points (§3.1) are indicated as vertical dark red lines. The left one at about $t_1^{\text{cand}} \approx 1.54$ is a local minimum of the posterior mean in between the red and blue point (note that the mean of the gradient belief in solid orange in the middle plot crosses through zero here). The right one at $t_2^{\text{cand}} = 4$ is a candidate for extrapolation. Bottom: Decision criterion in arbitrary scale: The expected improvement u_{EI} (Eq. 9) is shown in dashed light blue, the Wolfe probability p^{Wolfe} (Eq. 14 and Eq. 16) in light red and their decisive product in solid dark blue. For illustrative purposes all criteria are plotted for the whole t -space. In practice solely the values at t_1^{cand} and t_2^{cand} are computed, compared, and the candidate with the higher value of $u_{\text{EI}} \cdot p^{\text{Wolfe}}$ is chosen for evaluation. In this example this would be the candidate at t_1^{cand} .

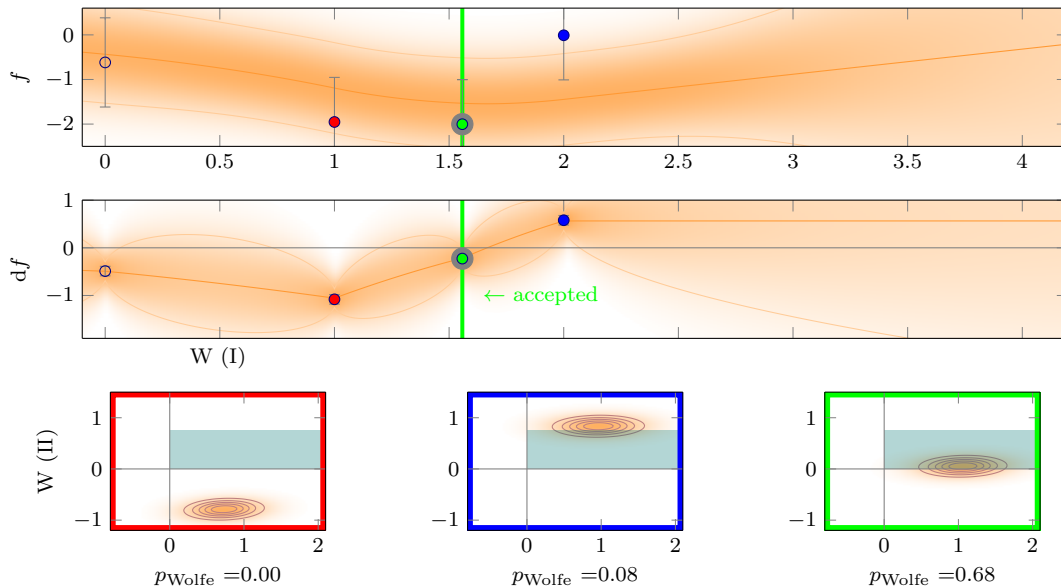


Figure 4: Illustration of *acceptance procedure*. Top: GP marginal posterior of function values. Posterior mean in solid orange and, two standard deviations in thinner solid orange, local pdf marginal as shading. The red, blue and green point are evaluations of the objective function, collected by the line search. Middle: GP marginal posterior of corresponding gradients. Colors same as in top plot. Bottom: Implied bivariate Gaussian belief over the validity of the Wolfe conditions (Eq. 11) at the red, blue and green point respectively. Points are considered acceptable if their Wolfe probability p_t^{Wolfe} (Eq. 14 and Eq. 16) is above a threshold $c_W = 0.3$ (§3.4.1). In the bottom plot this means that at least 30% of the orange 2D Gauss density must cover the dark green shaded area. Only the green point fulfills this condition and is therefore accepted.

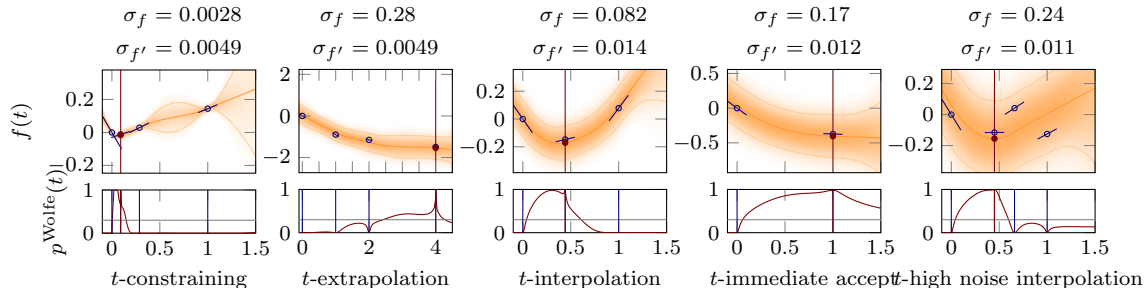


Figure 5: Curated snapshots of line searches (from N-I on MNIST), showing variability of the objective's shape and the decision process. Top row: GP marginal posterior of function values and evaluations, bottom row: approximate p^{Wolfe} (Eq. 14 and Eq. 16) over strong Wolfe conditions. Accepted point marked red.

The GP of Eq. 5 on f thus implies, at each value of t , a bivariate Gaussian distribution

$$p(a_t, b_t) = \mathcal{N} \left(\begin{bmatrix} a_t \\ b_t \end{bmatrix}; \begin{bmatrix} m_t^a \\ m_t^b \end{bmatrix}, \begin{bmatrix} C_t^{aa} & C_t^{ab} \\ C_t^{ba} & C_t^{bb} \end{bmatrix} \right), \quad (11)$$

$$\begin{aligned} \text{with } m_t^a &= \mu(0) - \mu(t) + c_1 t \mu'(0) \\ m_t^b &= \mu'(t) - c_2 \mu'(0) \end{aligned} \quad (12)$$

$$\begin{aligned} \text{and } C_t^{aa} &= \tilde{k}_{00} + (c_1 t)^2 \partial \tilde{k}_{00}^\partial + \tilde{k}_{tt} + 2[c_1 t (\tilde{k}_{00}^\partial - \partial \tilde{k}_{0t}^\partial) - \tilde{k}_{0t}^\partial] \\ C_t^{bb} &= c_2^2 \partial \tilde{k}_{00}^\partial - 2c_2 \partial \tilde{k}_{0t}^\partial + \partial \tilde{k}_{tt}^\partial \end{aligned} \quad (13)$$

$$C_t^{ab} = C_t^{ba} = -c_2 (\tilde{k}_{00}^\partial + c_1 t \partial \tilde{k}_{00}^\partial) + c_2 \partial \tilde{k}_{0t}^\partial + \partial \tilde{k}_{t0}^\partial + c_1 t \partial \tilde{k}_{0t}^\partial - \tilde{k}_{tt}^\partial.$$

The quadrant probability $p_t^{\text{Wolfe}} = p(a_t > 0 \wedge b_t > 0)$ for the Wolfe conditions to hold is an integral over a bivariate normal probability,

$$p_t^{\text{Wolfe}} = \int_{-\frac{m_t^a}{\sqrt{C_t^{aa}}}}^{\infty} \int_{-\frac{m_t^b}{\sqrt{C_t^{bb}}}}^{\infty} \mathcal{N} \left(\begin{bmatrix} a \\ b \end{bmatrix}; \begin{bmatrix} 0 \\ 0 \end{bmatrix}, \begin{bmatrix} 1 & \rho_t \\ \rho_t & 1 \end{bmatrix} \right) da db, \quad (14)$$

with correlation coefficient $\rho_t = C_t^{ab} / \sqrt{C_t^{aa} C_t^{bb}}$. It can be computed efficiently (Drezner and Wesolowsky, 1990), using readily available code⁵ (see Sections 3.5 and 3.6 for an analysis of memory and time overhead). The line search computes this probability for all evaluation nodes, after each evaluation. If any of the nodes fulfills the Wolfe conditions with $p_t^{\text{Wolfe}} > c_W$, greater than some threshold $0 < c_W \leq 1$, it is accepted and returned. If several nodes simultaneously fulfill this requirement, t of the most recently evaluated node (if available) or of the lowest $\mu(t)$ is returned. Section 3.4.1 below motivates fixing $c_W = 0.3$. The acceptance procedure is illustrated in Figure 4.

3.3.1 APPROXIMATION FOR STRONG CONDITIONS:

As noted in Section 2.1.1, deterministic optimizers tend to use the strong Wolfe conditions, which use $|f'(0)|$ and $|f'(t)|$. A precise extension of these conditions to the probabilistic setting is numerically taxing, because the distribution over $|f'|$ is a non-central χ -distribution, requiring customized computations. However, a straightforward variation to Eq. 14 captures the spirit of the strong Wolfe conditions, that large positive derivatives should not be accepted: Assuming $f'(0) < 0$ (i.e. that the search direction is a descent direction), the strong second Wolfe condition can be written exactly as

$$0 \leq b_t = f'(t) - c_2 f'(0) \leq -2c_2 f'(0). \quad (15)$$

The value $-2c_2 f'(0)$ is bounded to 95% confidence by

$$-2c_2 f'(0) \lesssim 2c_2 (|\mu'(0)| + 2\sqrt{\nabla'(0)}) =: \bar{b}. \quad (16)$$

Hence, an approximation to the strong Wolfe conditions can be reached by replacing the infinite upper integration limit on b in Eq. 14 with $(\bar{b} - m_t^b) / \sqrt{C_t^{bb}}$. The effect of this adaptation, which adds no overhead to the computation, is shown in Figure 2 as a dashed line.

⁵ e.g. <http://www.math.wsu.edu/faculty/genz/software/matlab/bvn.m>

3.4 Eliminating Hyper-parameters

As a black-box inner loop, the line search should not require any tuning by the user. The preceding section introduced six so-far undefined parameters: $c_1, c_2, c_W, \theta, \sigma_f, \sigma_{f'}$. We will now show that c_1, c_2, c_W , can be fixed by hard design decisions. θ can be eliminated by standardizing the optimization objective within the line search; and the noise levels can be estimated at runtime with low overhead for finite-sum objectives of the form in Eq. 1. The result is a parameter-free algorithm that effectively *removes* the one most problematic parameter from SGD—the learning rate.

3.4.1

Design Parameters c_1, c_2, c_W

Our algorithm inherits the Wolfe thresholds c_1 and c_2 from its deterministic ancestors. We set $c_1 = 0.05$ and $c_2 = 0.5$. This is a standard setting that yields a ‘lenient’ line search, i.e. one that accepts most descent points. The rationale is that the stochastic aspect of SGD is not always problematic, but can also be helpful through a kind of ‘annealing’ effect.

The acceptance threshold c_W is a new design parameter arising only in the probabilistic setting. We fix it to $c_W = 0.3$. To motivate this value, first note that in the noise-free limit, all values $0 < c_W < 1$ are equivalent, because p^{Wolfe} then switches discretely between 0 and 1 upon observation of the function. A back-of-the-envelope computation, assuming only two evaluations at $t = 0$ and $t = t_1$ and the same fixed noise level on f and f' (which then cancels out), shows that function values barely fulfilling the conditions, i.e. $a_{t_1} = b_{t_1} = 0$, can have $p^{\text{Wolfe}} \sim 0.2$ while function values at $a_{t_1} = b_{t_1} = -\epsilon$ for $\epsilon \rightarrow 0$ with ‘unlucky’ evaluations (both function and gradient values one standard-deviation from true value) can achieve $p^{\text{Wolfe}} \sim 0.4$. The choice $c_W = 0.3$ balances the two competing desiderata for precision and recall. Empirically (Fig. 5), we rarely observed values of p^{Wolfe} close to this threshold. Even at high evaluation noise, a function evaluation typically either clearly rules out the Wolfe conditions, or lifts p^{Wolfe} well above the threshold. A more in-depth analysis of c_1, c_2 , and c_W is done in the experimental Section 4.2.1.

3.4.2

Scale θ

The parameter θ of Eq. 4 simply scales the prior variance. It can be eliminated by scaling the optimization objective: We set $\theta = 1$ and scale $y_i \leftarrow (y_i - y_0)/|y'_0|, y'_i \leftarrow y'_i/|y'_0|$ within the code of the line search. This gives $y(0) = 0$ and $y'(0) = -1$, and typically ensures the objective ranges in the single digits across $0 < t < 10$, where most line searches take place. The division by $|y'_0|$ causes a non-Gaussian disturbance, but this does not seem to have notable empirical effect.

3.4.3

Noise Scales $\sigma_f, \sigma_{f'}$

The likelihood (3) requires standard deviations for the noise on both function values (σ_f) and gradients ($\sigma_{f'}$). One could attempt to learn these across several line searches. However, in exchangeable models, as captured by Eq. 1, the variance of the loss and its gradient can

be estimated directly within the mini-batch, at low computational overhead—an approach already advocated by Schaul et al. (2013). We collect the empirical statistics

$$\hat{S}(x) := \frac{1}{m} \sum_j^m \ell^2(x, y_j), \quad \text{and} \quad \hat{\nabla}S(x) := \frac{1}{m} \sum_j^m \nabla \ell(x, y_j).^2 \quad (17)$$

(where $.^2$ denotes the element-wise square) and estimate, at the beginning of a line search from x_k ,

$$\sigma_f^2 = \frac{1}{m-1} \left(\hat{S}(x_k) - \hat{\mathcal{L}}(x_k)^2 \right) \quad \text{and} \quad \sigma_{f'}^2 = s_i.^{2\top} \left[\frac{1}{m-1} \left(\hat{\nabla}S(x_k) - (\nabla \hat{\mathcal{L}}).^2 \right) \right]. \quad (18)$$

This amounts to the cautious assumption that noise on the gradient is independent. We finally scale the two empirical estimates as described in Section §3.4.2: $\sigma_f \leftarrow \sigma_f/|y'(0)|$, and ditto for $\sigma_{f'}$. The overhead of this estimation is small if the computation of $\ell(x, y_j)$ itself is more expensive than the summation over j . In the neural network examples N-I and N-II of the experimental Section 4, the additional steps added only $\sim 1\%$ cost overhead to the evaluation of the loss. A more general statement about memory and time requirements however can be found in Sections 3.5 and 3.6. Of course, this approach requires a mini-batch size $m > 1$. For single-sample mini-batches, a running averaging could be used instead (single-sample mini-batches are not necessarily a good choice. In our experiments, for example, vanilla SGD with batch size 10 converged faster in wall-clock time than unit-batch SGD). Estimating noise separately for each input dimension captures the often inhomogeneous structure among gradient elements, and its effect on the noise along the projected direction. For example, in deep models, gradient noise is typically higher on weights between the input and first hidden layer, hence line searches along the corresponding directions are noisier than those along directions affecting higher-level weights. A detailed description of the noise estimator can be found in Appendix A.

3.4.4 PROPAGATING STEP SIZES BETWEEN LINE SEARCHES

As will be demonstrated in §4, the line search can find good step sizes even if the length of the direction s_i (which is proportional to the learning rate α in SGD) is mis-scaled. Since such scale issues typically persist over time, it would be wasteful to have the algorithm re-fit a good scale in each line search. Instead, we propagate step lengths from one iteration of the search to another: We set the initial search direction to $s_0 = -\alpha_0 \nabla \hat{\mathcal{L}}(x_0)$ with some initial learning rate α_0 . Then, after each line search ending at $x_i = x_{i-1} + t_* s_i$, the next search direction is set to $s_{i+1} = -\alpha_{\text{ext}} \cdot t_* \alpha_0 \nabla \hat{\mathcal{L}}(x_i)$ (with $\alpha_{\text{ext}} = 1.3$). Thus, the next line search starts its extrapolation at 1.3 times the step size of its predecessor (Section 4.2.2 for details).

Remark on convergence of SGD with line searches: We note in passing that it is straightforward to ensure that SGD instances using the line search inherit the convergence guarantees of SGD: Putting even an extremely loose bound $\bar{\alpha}_i$ on the step sizes taken by the i -th line search, such that $\sum_i^\infty \bar{\alpha}_i = \infty$ and $\sum_i^\infty \bar{\alpha}_i^2 < \infty$, ensures the line search-controlled SGD converges in probability (Robbins and Monro, 1951).

3.5 Computational Time Overhead

The line search routine itself has little memory and time overhead, most importantly being independent of the dimensionality of the optimization problem. After every call of the objective function the 2-dimensional GP (§3.1) needs to be updated which at most is at the cost of inverting a $2N \times 2N$ -matrix, where N normally is equal to 1, 2, or 3 but never > 10 . In addition the bivariate normal integral p_t^{Wolfe} of Eq. 14 needs to be computed at most N times. On a laptop, one evaluation of p_t^{Wolfe} costs about 100 microseconds. For the choice among proposed candidates (§3.2), again at most N , for each, we need to evaluate p_t^{Wolfe} and $u_{\text{EI}}(t)$ (Eq. 9) where the latter comes at the expense of evaluating two error functions. Since all of these computations have a fixed cost (in total some milliseconds on a laptop), the relative overhead becomes less the more expensive the evaluation of $\nabla \hat{\mathcal{L}}(x)$.

The largest overhead actually lies outside of the actual line search routine. In case the noise levels σ_f and $\sigma_{f'}$ is not known, we need to estimate them. The approach we took is described in Section 3.4.3 where the variance of $\nabla \hat{\mathcal{L}}$ is estimated using the sample variance of the minibatch, each time the objective function is called. Since in this formulation the variance estimation is about half as expensive as one backward pass of the net, the time overhead depends on the relative cost of the feed forward and backward passes (Balles et al., 2016). If forward and backward pass are the same cost, the most straightforward implementation of the variance estimation would make each function call 1.25 times as expensive.⁶ At the same time though, *all* exploratory experiments which very considerably increase the time spend when using SGD with a hand tuned learning rate schedule need not be performed anymore. In Section 4.1 we will also see that SGD using the probabilistic line search often needs less function evaluations to converge, which might lead to overall faster convergence in wall clock time than classic SGD in a single run.

3.6 Memory Requirement

Vanilla SGD at all times keeps around the current optimization parameters $x \in \mathbb{R}^D$ and the gradient vector $\nabla \hat{\mathcal{L}}(x) \in \mathbb{R}^D$. In addition to this the probabilistic line search needs to store the estimated gradient variances $\Sigma'(x) = (1 - m)^{-1}(\nabla \hat{S}(x) - \nabla \hat{\mathcal{L}}(x))^2$ (18) of same size. The memory requirement of SGD+PROBLS is thus comparable to ADAGRAD or ADAM. If combined with a search direction other than SGD always one additional vector of size D needs to be stored.

4. Experiments

This section reports on an extensive set of experiments to characterise and test the line search. The overall evidence from these tests is that the line search performs well and is relatively insensitive to the choice of its internal hyper-parameters as well the mini-batch

6. It is desirable to decrease this value in the future reusing computation results or by approximation but this is beyond this discussion.

size. We performed experiments on two different artificial neural networks and on two well known datasets MNIST⁷ and CIFAR-10⁸.

- N-I: fully connected net with 1 hidden layer and 800 hidden units + biases, and 10 output units, sigmoidal activation functions and a cross entropy loss. Structure without biases: 784-800-10. Many authors used similar nets and reported performances.⁷
- N-II: fully connected net with 3 hidden layers and 10 output units, tanh-activation functions and a squared loss. Structure without biases: 784-1000-500-250-10. Similar nets were also used for example in Martens (2010) and Sutskever et al. (2013).

In the text and figures, SGD using the probabilistic line search will occasionally be denoted as SGD+PROBLS. Section 4.1 contains experiments on the sensitivity to varying gradient noise levels (mini-batch sizes) performed on both N-I and N-II. Section 4.2 discusses sensitivity to the hyper parameters choices introduced in Section 3.4 and Section 4.3 contains additional diagnostics on step size statistics. Each single experiment was performed 10 times with different random seeds that determined the starting weights and the mini-batch selection and seeds were shared across all experiments. We report all results of the 10 instances as well as means and standard deviations.

4.1 Varying Mini-batch Sizes

The level of noise of the gradient estimate $\nabla\hat{\mathcal{L}}(x)$ and the loss $\hat{\mathcal{L}}(x)$ is determined by the mini-batch size m and ultimately there should exist an optimal m that maximizes the optimizer’s performance in wall-clock-time. In practice of course the cost of computing $\nabla\hat{\mathcal{L}}(x)$ and $\hat{\mathcal{L}}(x)$ is not necessarily linear in m since it is upper bounded by the memory capacity of the hardware used. Thus we test the line search on four different mini-batch sizes $m = 10, 100, 200$ and 1000 which correspond to increasing signal to noise ratios on the nets N-I and N-II on both, MNIST and CIFAR-10 with the default hyper parameter setting discussed in Sections 3.4 and 4.2. We compare to SGD-runs using a fixed step size (which is typical for the architectures used) and an annealed step size with annealing schedule $\alpha_t = \alpha_0/t$. Because optimizers using the annealed step size performed much worse than SGD+fixed step size, we will only report the latter results in the plots.⁹ Since classic SGD without the line search needs a hand crafted learning rate we search on an exhaustive logarithmic grid of $\alpha_{\text{SGD}}^{\text{N-I}} = [1 \cdot 10^{-5}, 5 \cdot 10^{-5}, 1 \cdot 10^{-4}, 5 \cdot 10^{-4}, 1 \cdot 10^{-3}, 5 \cdot 10^{-3}, 1 \cdot 10^{-2}, 5 \cdot 10^{-2}, 1 \cdot 10^{-1}, 5 \cdot 10^{-1}]$ for N-II and $\alpha_{\text{SGD}}^{\text{N-II}} = [\alpha_{\text{SGD}}^{\text{N-I}}, 1.0, 1.5, 2.0, 2.5, 3.0, 3.5, 4.0]$ for N-I. We run 10 different initialization for each learning rate, each mini-batch size and each net and dataset combination $((10 + 17) \cdot 10 \cdot 4 \cdot 2 \cdot 2 = 4320$ runs in total) for a budget of 40 000 (MNIST) and 10 000 (CIFAR-10) steps and report all numbers. Then we perform the same experiments using the same seeds and setups with SGD using the probabilistic line search and compare the results. For SGD+PROBLS, α_{SGD} is the initial learning rate which is used in the very first step. After that the line search automatically adapts the learning rate, showing no significant sensitivity to its initialization.

7. <http://yann.lecun.com/exdb/mnist/>

8. <http://www.cs.toronto.edu/~kriz/cifar.html>. Like other authors, we only used the “batch 1” sub-set of CIFAR-10.

9. an example of annealed step size performance can be found in Mahsereci and Hennig (2015).

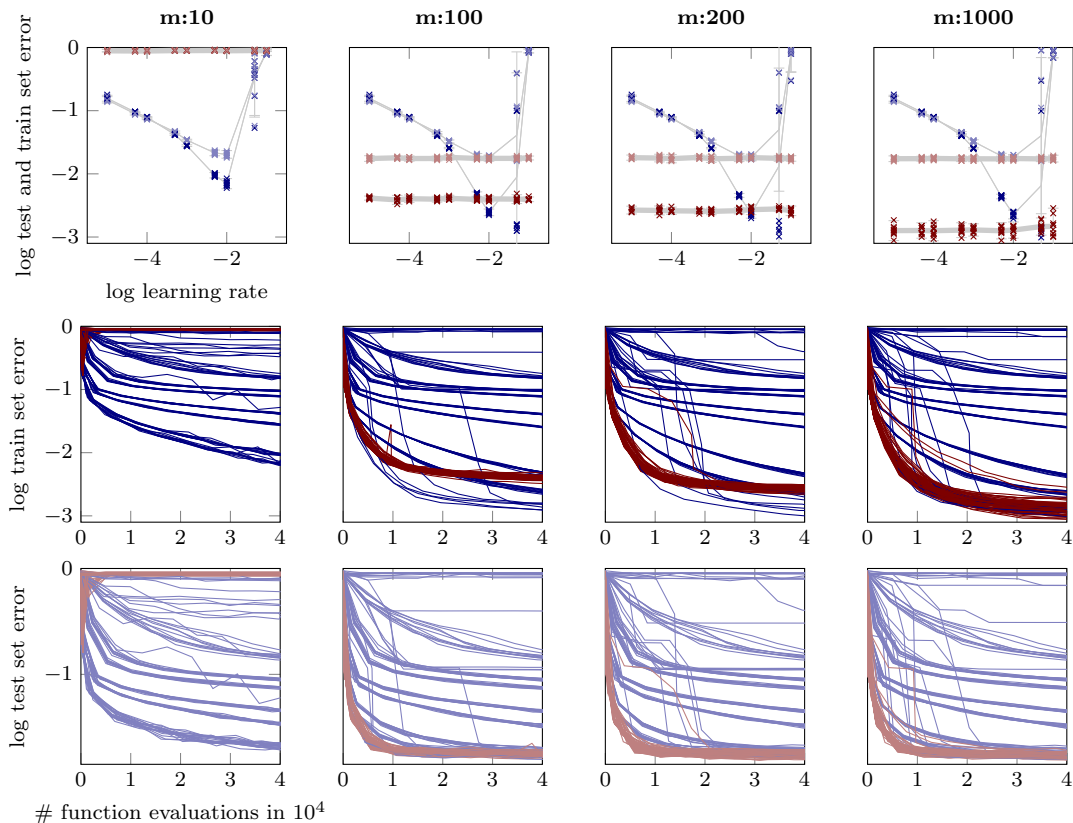


Figure 6: Performance of N-II on MNIST for *varying mini-batch sizes*. Top: final logarithmic test set and train set error after 40 000 function evaluations of training versus a large range of learning rates each for 10 different initializations. SGD-runs with fixed learning rates are shown in light blue (test set) and dark blue (train set), SGD+PROBLS-runs in light red (test set) and dark red (train set). Means and two standard deviations for each of the 10 runs are drawn in gray. Columns from left to right refer to different mini-batch sizes m of 10, 100, 200 and 1000 which correspond to decreasing relative noise in the gradient observations. Not surprisingly the performance of SGD-runs with a fixed step size are very sensitive to its choice. SGD using the probabilistic line search however adapts initially mis-scaled step sizes and performs well across the whole range of initial learning rates. The middle and bottom plots show the evolution of the logarithmic test and train set error respectively for all SGD-runs and SGD+PROBLS-runs versus # function evaluations (colors as in top plot). For min-batch sizes of $m = 100, 200$ and 1000 *all* instances of SGD using the probabilistic line search reach the same best test set error. Similarly a good train set error is reached very fast by SGD+PROBLS. Only very few instances of SGD with a fixed learning rate reach a better train set error (and this advantage usually does not translate to test set error). For very small mini-batch sizes ($m = 10$ and first column in the plot) the line search becomes unstable with this architecture, possibly because of the variance estimation becoming too inaccurate (see Appendix A).

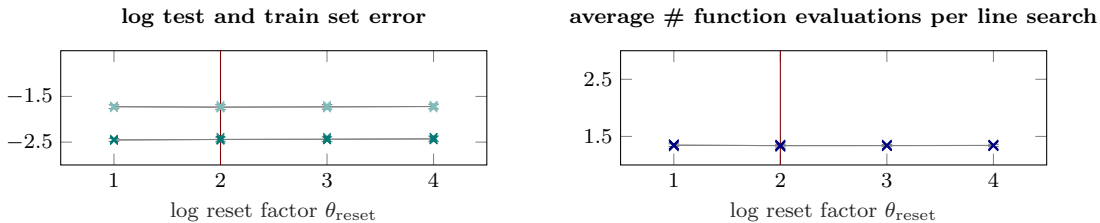


Figure 7: *Sensitivity to varying hyper parameters θ_{reset} .* Plot and color coding as in Figure 8. Adopted parameter in dark red at $\theta_{\text{reset}} = 100$. Resetting the GP scale occurs very rarely. For example for $\theta_{\text{reset}} = 100$ the reset occurred in 0.02% of all line searches.

Results training N-II on MNIST are shown in Figure 6, N-I on MNIST in Figure 12 and N-II and N-I on CIFAR-10 in 13 and 14 respectively. Note that all instances (SGD and SGD+PROBLS) get the same computational budget (number of mini-batch evaluations) and not the same number of optimization steps. The latter would favour the probabilistic line search since on average a bit more than one mini-batch is evaluated per step. Likewise all plots show performance measure versus the number of mini-batch evaluations which is proportional to the computational cost.

All plots show similar results: While classic SGD is sensitive to the learning rate choice, the line search-controlled SGD performs as good, close to, or sometimes even better than the (in practice unknown) optimal classic SGD instance. In Figure 6 for example SGD+PROBLS converges much faster to a good test set error than the best classic SGD instance. In all experiments, across a reasonable range of mini-batch sizes m and of initial α_{SGD} values, the line search quickly identified good step sizes α_t , stabilized the training, and progressed efficiently, reaching test set errors similar to those reported in the literature for tuned versions of this kind of architecture on these datasets, effectively removing the need for exploratory experiments and learning-rate tuning.

4.2 Sensitivity to Design Parameters

Most if not all numerical methods make implicit or explicit choices about their hyper parameters. Most of these are never seen by the user since they are either estimated at run time or set by design to a fixed, approximately insensitive value. Well known examples are the discount factor in ordinary differential equation solvers (Hairer et al., 1987, §2.4) or the Wolfe parameters c_1 and c_2 of classic line searches (§3.4.1). The probabilistic line search inherits the Wolfe parameters c_1 and c_2 from its classical counterpart as well as introducing two more, the Wolfe threshold c_W and the extrapolation factor α_{ext} . c_W does not appear in the classical formulation since the objective function can be evaluated exactly and the Wolfe probability is binary (either fulfilled or not). While c_W therefore is a natural consequence of allowing the line search to model noise explicitly, the extrapolation factor α_{ext} is the result of the line search favoring shorter steps, which we will discuss below in more detail, but most prominently because of bias in the line search’s first gradient observation.

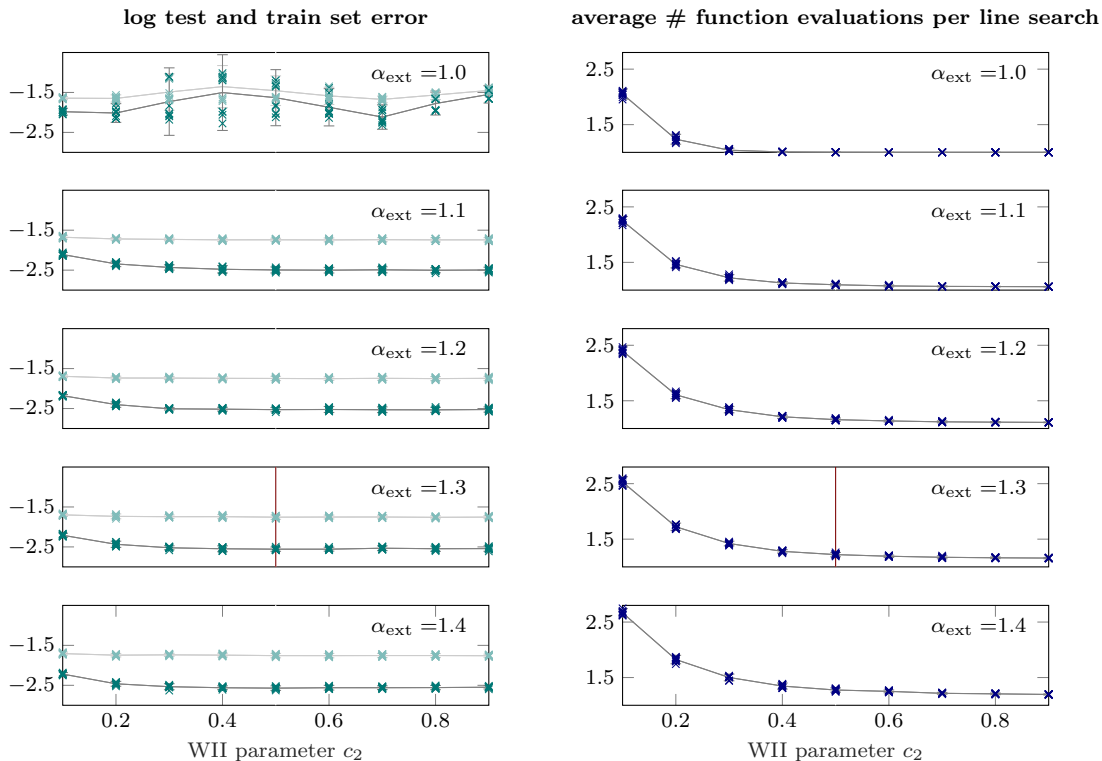


Figure 8: *Sensitivity to varying hyper parameters c_2 , and α_{ext} (§3.4, §4.2).* Runs were performed training N-II on MNIST of with mini-batch size $m = 200$. For each parameter setting 10 runs with different initializations were performed. Left column: logarithmic test set error (light green) and train set error (dark green) after 40 000 function evaluations. Mean and \pm two standard deviations of the 10 runs in gray. Right Column: average number of function evaluations per line search. A low number indicates an efficient line search procedure (perfect efficiency at 1). For most parameter combinations this lies around $\approx 1.3 - 1.5$. Only at extreme parameter values, for example $\alpha_{\text{ext}} = 1.0$, which amounts to no extrapolation at all in between successive line searches, the line search becomes unstable. The hyper parameters adopted in the line search implementation are indicated as vertical dark red line at $\alpha_{\text{ext}} = 1.3$ and $c_2 = 0.5$.

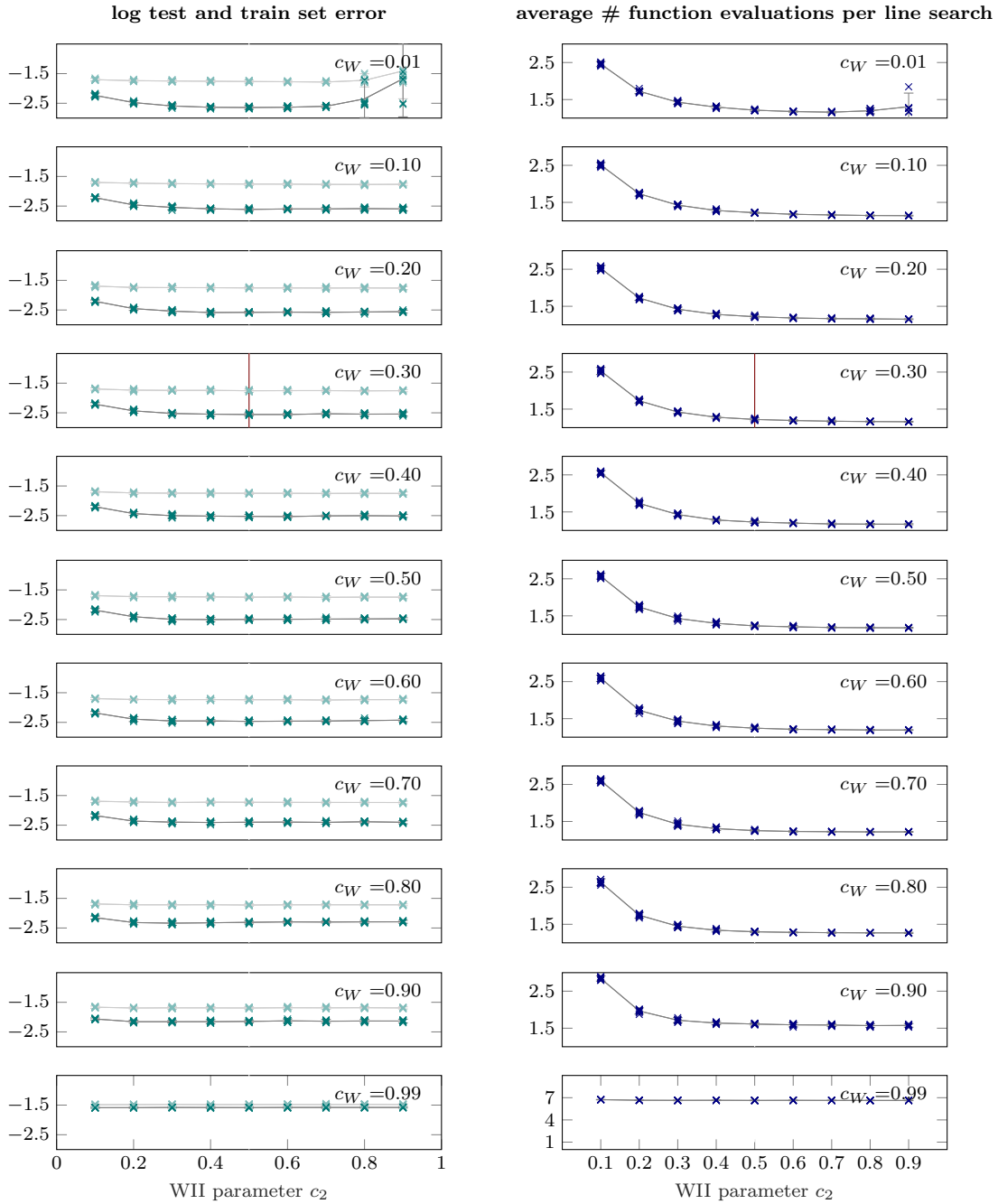


Figure 9: *Sensitivity to varying hyper parameters c_2 , and c_W (§3.4).* Plot and color coding as in Figure 8 but this time for varying c_W instead of α_{ext} . Right Column: Again a low number indicates an efficient line search procedure (perfect efficiency at 1). For most parameter combinations this lies around $\approx 1.3 - 1.5$. Only at extreme parameter values for example $c_W = 0.99$, which amounts to imposing nearly absolute certainty about the Wolfe conditions, the line search becomes less efficient, though still does not break. Adopted parameters again in dark red at $c_W = 0.3$ and $c_2 = 0.5$

In the following we will give an intuition about the task of the most influential design parameters c_2 , c_W , and α_{ext} , discuss how they affect the probabilistic line search, and validate good design choices through exploring the parameter space and showing insensitivity to most of them. All experiments on hyper parameter sensitivity were performed training N-II on MNIST with mini-batch size $m = 200$. For a full search of the parameter space c_W - c_2 - α_{ext} we performed 4950 runs in total using 495 different parameter combinations. All results are reported.

4.2.1 WOLFE II PARAMETER c_2 AND WOLFE THRESHOLD c_W

As described in Section 3.4, c_2 encodes the strictness of the curvature condition W-II. Pictorially speaking a larger c_2 extends the range of acceptable gradients (green shaded are in the lower part of Figure 4) and will lead to a lenient line search while a smaller value of c_2 will shrink this area leading to a stricter line search. c_W controls how certain we want to be that the Wolfe conditions are actually fulfilled. In the extreme case of complete uncertainty about the collected gradients and function values ($\sigma_f, \sigma_{f'} \rightarrow \infty$) p^{Wolfe} will be always < 0.25 if the strong Wolfe conditions are imposed. In the limit of certain observations ($\sigma_f, \sigma_{f'} \rightarrow 0$) p^{Wolfe} is binary and reverts to the classic Wolfe criteria. An overly strict line search therefore (e.g. $c_W = 0.99$ and/ or $c_2 = 0.1$) will still be able to optimize the objective function well, but will waste evaluations at the expense of efficiency. Figure 9 explores the c_2 - c_W parameters space (while keeping α_{ext} fixed at 1.3). The left column shows final test and train set error, the right column the average number of function evaluations per line search, both versus different choices of Wolfe parameter c_2 . The left column thus shows overall performance of the optimizer while the right column is representative for the efficiency of the line search. Intuitively a line search which is minimally invasive (only corrects the learning rate when it is really necessary) is preferred. Rows in Figure 9 show the same plot for different choices of the Wolfe threshold c_W .

The effect of strict c_2 can be observed clearly in Figure 9 where for smaller values of $c_2 < \approx 0.2$ the average number of function evaluations spend in one line search goes up slightly in comparison to looser restrictions on c_2 while still a very good performance is reached in terms of train and test set error. Likewise the last row of Figure 9 for the extreme value of $c_W = 0.99$ (demanding 99% certainty about the validity if the Wolfe conditions) shows significant loss in efficiency having an average number of 7 function evaluations per line search but still does not break. Lowering this threshold a bit to 90% increases the efficiency of the line search to be nearly optimal again.

Ideally we want to trade off the desirata of being strict enough to reject steps that prevent the optimizer to converge, but being lenient enough to allow all other reasonable steps, thus increasing efficiency. The values $c_W = 0.3$ and $c_2 = 0.5$ adopted in our current implementation are marked as dark red vertical lines in Figure 9.

4.2.2 EXTRAPOLATION FACTOR α_{EXT}

The extrapolation parameter α_{ext} introduced in Section 3.4.4 pushes the line search to try a larger learning rate first than the one which was accepted in the previous step. Figure 8 is structured like Figure 9 but this time explores the line search sensitivity in the c_2 - α_{ext} parameter space (abscissa and rows respectively) while keeping c_W fixed at 0.3. Unless we

choose $\alpha_{\text{ext}} = 1.0$ (no step size increase between steps) in combination with a lenient choice of c_2 the line search performs well. For now we adopt $\alpha_{\text{ext}} = 1.3$ as default value which again is shown as dark red vertical line in Figure 8.

The introduction of α_{ext} is a necessity and well-working fix because of a few shortcomings of the current design. First the curvature condition W-II is the single condition that prevents too small steps and pushes optimization progress. On the other hand both W-I and W-II simultaneously penalize too large steps (see Figure 1 for a sketch). This is not a problem in case of deterministic observation ($\sigma_f, \sigma_{f'} \rightarrow 0$) where W-II undoubtedly decides if a gradient is still too negative. Unless W-II is chosen very tightly (small c_2) or c_W unnecessarily large (both choices, as discussed above, are undesirable since inefficient), in the presence of noise, p^{Wolfe} will thus be more reliable in preventing overshooting than pushing progress. The first row of Figure 8 illustrates this behavior where the performance drops somewhat if no extrapolation is done ($\alpha_{\text{ext}} = 1.0$) in combination with a looser version of W-II (larger c_2).

Another factor that contributes towards accepting small rather than larger learning rates is a bias introduced in the first observation of the line search at $t = 0$. Observations $y'(t)$ that the GP gets to see are projections of the gradient sample $\nabla \hat{\mathcal{L}}(t)$ onto the search direction $s = -\nabla \hat{\mathcal{L}}(0)$. Since the first observations $y'(0)$ is computed from the same mini-batch as the search direction (not doing this would double the optimizer’s cost) an inevitable bias is introduced of approximate size of $\cos^{-1}(\gamma)$ (where γ is the expected angle between gradient evaluations from two independent mini-batches at $t = 0$). Since the scale parameter θ of the Wiener process is implicitly set by $y'(0)$ (§3.4.2) the GP becomes more uncertain at unobserved points than it needs to be or alternatively expects the 1D-gradient to cross zero at smaller steps and thus underestimating a potential learning rate. The posterior at observed positions however is little affected. The over-estimation of θ rather pushes the posterior towards the likelihood (since there is less model to trust) and thus still gives a reliable measure for $f(t)$ and $f'(t)$. The effect on the Wolfe conditions is similar. With $y'(0)$ biased towards larger values, the Wolfe conditions, which measure the drop in projected gradient norm, are thus prone to accept larger gradients combined with smaller function values, which again is met by making small steps. Ultimately though, since candidate points at $t^{\text{cand}} > 0$ that are currently queried for acceptance, are always observed and unbiased, this can be controlled by an appropriate design of the Wolfe factor c_2 (§3.4.1 and §4.2.1) and of course α_{ext} .

4.2.3 FULL HYPER PARAMETER SEARCH: c_W - c_2 - α_{EXT}

An exhaustive performance evaluation on the whole c_W - c_2 - α_{ext} -grid is shown in Appendix C in Figures 15-19 and Figures 20-30. As discussed above it shows the necessity of introducing the extrapolation parameter α_{ext} and shows slightly less efficient performance for obviously undesirable parameter combinations. In a large volume of the parameter space and most importantly in the vicinity of the chosen design parameters the line search performance is stable and comparable to carefully hand tuned learning rates.

4.2.4 SAFEGUARDING MIS-SCALED GPS: θ_{RESET}

For completeness an additional experiment was performed on the threshold parameter which is denoted by θ_{reset} in the pseudo-code (Appendix D) and safeguards against GP mis-scaling.

The introduction of noisy observations necessitates to model the variability of the 1D-function which is described by the kernel scale parameter θ (§3.4.2). Setting this hyper parameter is implicitly done by scaling the observation input assuming a similar scale than in the previous line search (§3.4.2). If for some reason the previous line search accepted an unexpectedly large or small step (what this means is encoded in θ_{reset}) the GP scale θ for the next line search is reset to an exponential running average of previous scales (α_{stats} in the pseudo-code). This occurs very rarely (for the default value $\theta_{\text{reset}} = 100$ the reset occurred in 0.02% of all line searches), but is necessary to safeguard against extremely mis-scaled GP’s. θ_{reset} therefore is not part of the probabilistic line search model as such, but prevents GP-scaling which is way off due to some unlucky observation or sudden extreme change in the learning rate. Figure 7 shows performance of the line search for $\theta_{\text{reset}} = 10, 100, 1000$ and 10 000 showing no significant performance change. We adopted $\theta_{\text{reset}} = 100$ in our implementation since this is the expected and desired multiplicative (inverse) factor to maximally vary the learning rate in one single step.

4.3 Candidate Selection and Learning Rate Traces

In the current implementation of the probabilistic line search the choice among candidates for evaluation is done by evaluating a utility function $u_{\text{EI}}(t_i^{\text{cand}}) \cdot p^{\text{Wolfe}}(t_i^{\text{cand}})$ at every candidate point t_i^{cand} , then choosing the one with the highest value for evaluation of the objective (§3.2). The Wolfe probability p^{Wolfe} actually encodes precisely what kind of point we want to find and incorporates both W-I and W-II, conditions to the function value *and* to the gradient (§3.3). However p^{Wolfe} does not have very desirable exploration properties. Since the uncertainty of the GP grows to ‘the right’ of the last observation, the Wolfe probability quickly drops to a low approximately constant value there (Figure 3). Also p^{Wolfe} is partially allowing for undesirably short steps (§4.2.2). The expected improvement u_{EI} on the other hand is a well studied acquisition function of Bayesian optimization trading off exploration and exploitation. It aims to globally find a point with a function value lower than a current best guess. Though this is a desirable property also for the probabilistic line search, it is lacking the information that we are seeking a point that also fulfills the W-II curvature condition as well. This is evident in Figure 3 where p^{Wolfe} significantly drops at points where the objective function is already evaluated but u_{EI} does not. In addition we do not need to explore the positive t space to an extend, the expected improvement suggests since the aim of a line search is just to find a good, acceptable point at positive t and not the globally best one. The product of both utilities $u_{\text{EI}} \cdot p^{\text{Wolfe}}$ is thus a trade-off between exploring enough, but still preventing too much exploitation in obviously undesirable regions. In practice, though, we found that all three choices ((i) $u_{\text{EI}} \cdot p^{\text{Wolfe}}$, (ii) u_{EI} only, (iii) p^{Wolfe} only) perform comparable. Figure 10 compares all three utility choices by training of N-II on MNIST with mini-batch size $m = 200$ and default design parameters. The top plot shows the evolution of the logarithmic test and train set error (for plot and color description see Figure caption). All test and train set error curves respectively bundle up. The choice of utility function thus does not change the performance here.

Rows 2-4 of Figure 10 show learning rate traces of a single seed. All three curves show very similar global behavior. First the learning rate grows, then drops again, to finally settle around the best found constant learning rate. This is intriguing since *on average* a

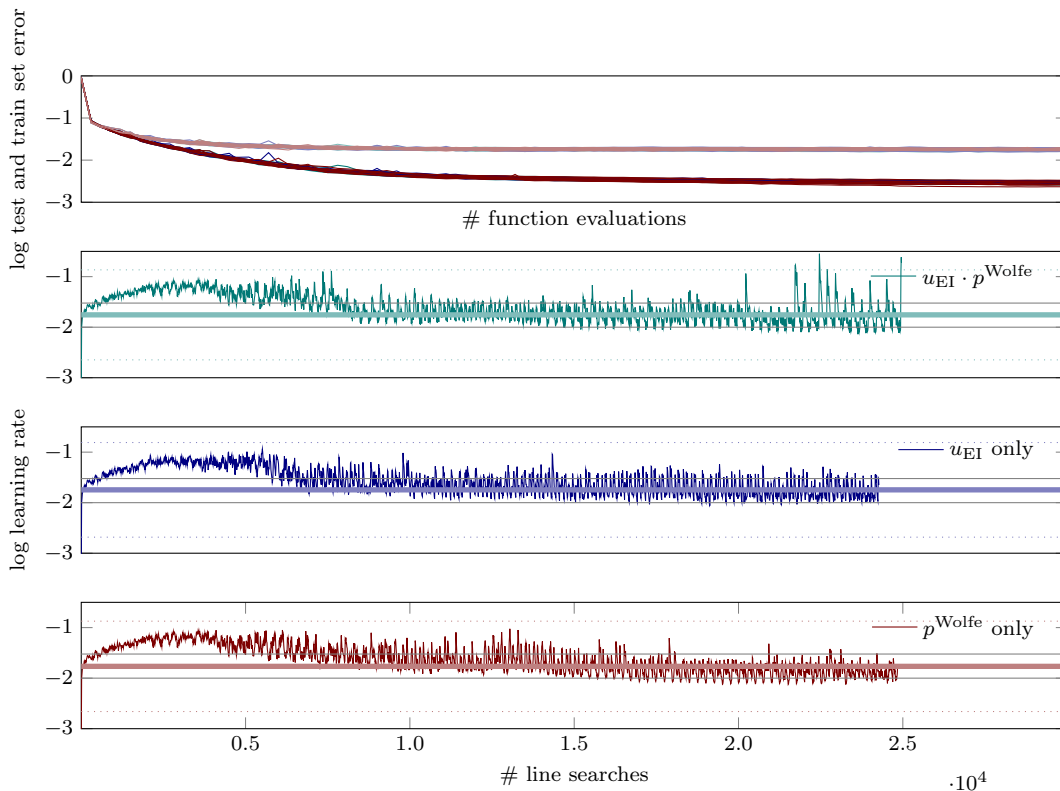


Figure 10: *Different choices of utility function* (§3.2). We compare between using expected improvement u_{EI} (blue), the Wolfe probability p^{Wolfe} (red) and their product $u_{\text{EI}} \cdot p^{\text{Wolfe}}$ (green) which is the default in our code. All runs are performed training N-II on MNIST with mini-batch size $m = 200$ and default design parameters. Top: evolution of the logarithmic test and train set error. Different lines of the same color correspond to different seeds. All test and train set error curves respectively bundle up. The choice of utility function thus does not change the performance here. Rows 2-4: show learning rate traces of a single seed (colors same as in top plot). For plotting purposes the curves were smoothed and thinned out. The thick light green, light red and light blue horizontal lines show the mean of the raw (non-smoothed) values of accepted learning rates across the whole optimization process, the dotted lines show \pm two standard deviations and the gray solid lines mark a range of well performing constant learning rates. All three curves show very similar global behavior. First the learning rate grows, then drops again, to finally settle around the best found constant learning rate. See main text for more detail.

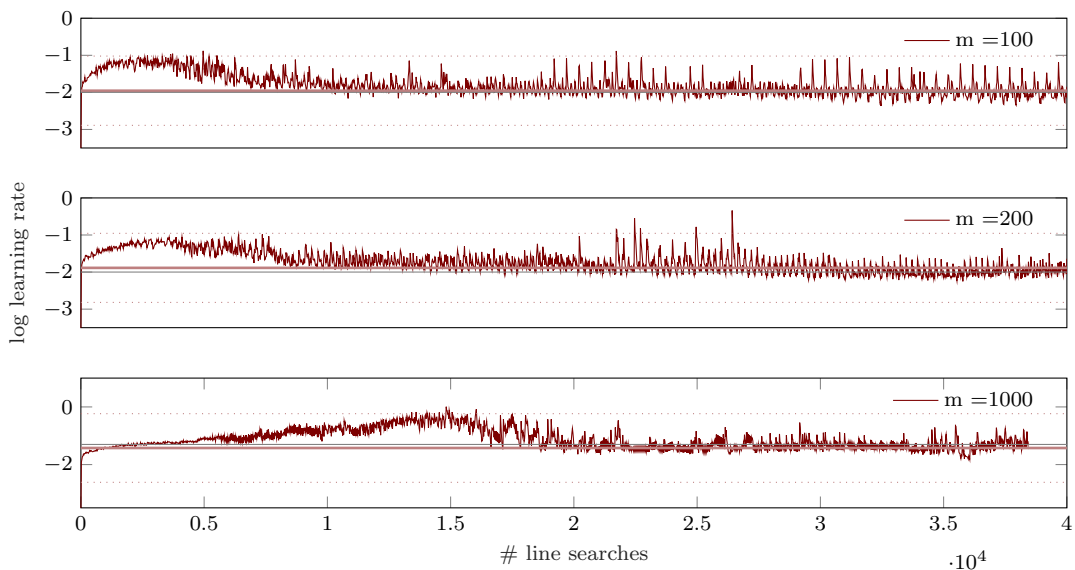


Figure 11: Traces of *accepted logarithmic learning rates*. All runs are performed training N-II on MNIST with default design parameters. Different rows show the same plot for different mini-batch sizes of $m = 100, 200$ and 1000 . For plotting purposes the curves were smoothed and thinned out. The thick light red horizontal line shows the mean of the raw (non-smoothed) values of accepted learning rates across the whole optimization process, the dotted lines show \pm two standard deviations and the gray solid line marks a well performing constant learning rate. All three curves show very similar global behavior for this architecture. First the learning rate grows, then drops again, to finally settle around the best found constant learning rate. For the largest mini-batch size $m = 1000$ (last row) the probabilistic line search accepts a larger learning rate (in average and absolute value) than for the smaller mini-batch sizes $m = 100$ and 200 , which is in agreement with practical experience theoretical findings.

larger learning rate seems to be better at the beginning of the optimization process, then later dropping again to a smaller, *in average* constant one. This might also explain why SGD+PROBLS in the first part of the optimization progress outperforms vanilla SGD (Figure 6). Runs, though that use just a tad larger constant learning rates than the best performing constant one (above the gray horizontal lines in Figure 10) were failing after a few steps. This shows that there is some non-trivial adaptation going on, not just globally, but locally at every step.

In addition Figure 11 shows traces of accepted learning rates for *different mini-batch sizes* (see figure caption for experiment details). Again the global behavior is qualitatively similar for all three mini-batch sizes on the given architecture N-II on MNIST. Also, for the largest mini-batch size $m = 1000$ (last row of Figure 11) the probabilistic line search accepts a larger learning rate (in average and in absolute value) than for the smaller mini-batch sizes $m = 100$ and 200 , which is in agreement with practical experience and theoretical findings.

5. Conclusion

The line search paradigm widely accepted in deterministic optimization can be extended to noisy settings. Our design combines existing principles from the noise-free case with ideas from Bayesian optimization, adapted for efficiency. We arrived at a lightweight “black-box” algorithm that exposes no parameters to the user. Our method is complementary to, and can in principle be combined with, virtually all existing methods for stochastic optimization that adapt a step *direction* of fixed *length*. Empirical evaluations suggest the line search effectively frees users from worries about the choice of a learning rate: Any reasonable initial choice will be quickly adapted and lead to close to optimal performance. Our matlab implementation can be found at <http://tinyurl.com/probLineSearch>.

Acknowledgments

Thanks to Jonas Jaszkwic who prepared the base of the pseudo-code and to Lukas Balles for helpful discussions.

Appendix A. – Noise Estimation

Section 3.4.3 introduced the statistical variance estimators

$$\begin{aligned}\Sigma'(x) &= (1 - m)^{-1}(\nabla\hat{S}(x) - \nabla\hat{\mathcal{L}}(x)).^2 \\ \Sigma(x) &= (1 - m)^{-1}(\hat{S}(x) - \hat{\mathcal{L}}(x)).^2\end{aligned}\tag{19}$$

of the function and gradient estimate $\hat{\mathcal{L}}(x)$ and $\nabla\hat{\mathcal{L}}(x)$ at position x . The underlying assumption is that $\hat{\mathcal{L}}(x)$ and $\nabla\hat{\mathcal{L}}(x)$ are distributed according to

$$\begin{bmatrix} \hat{\mathcal{L}}(x) \\ \nabla\hat{\mathcal{L}}(x) \end{bmatrix} \sim \mathcal{N} \left(\begin{bmatrix} \hat{\mathcal{L}}(x) \\ \nabla\hat{\mathcal{L}}(x) \end{bmatrix}; \begin{bmatrix} \mathcal{L}(x) \\ \nabla\mathcal{L}(x) \end{bmatrix}, \begin{bmatrix} \Sigma(x) & 0_{D \times 1} \\ 0_{1 \times D} & \text{diag } \Sigma'(x) \end{bmatrix} \right)\tag{20}$$

which implies Eq (3)

$$\begin{bmatrix} \hat{\mathcal{L}}(x) \\ s(x)' \cdot \nabla\hat{\mathcal{L}}(x) \end{bmatrix} = \begin{bmatrix} y(x) \\ y'(x) \end{bmatrix} \sim \mathcal{N} \left(\begin{bmatrix} y(x) \\ y'(x) \end{bmatrix}; \begin{bmatrix} f(x) \\ f'(x) \end{bmatrix}, \begin{bmatrix} \sigma_f(x) & 0 \\ 0 & \sigma_{f'}(x) \end{bmatrix} \right).\tag{21}$$

where $s(x)$ is the possibly new search direction at x . This is an approximation since the true covariance matrix is in general not diagonal. A better estimator for the projected gradient noise would be (dropping x from the notation)

$$\begin{aligned}\eta_{f'} &= s^\top \left[\frac{1}{m-1} \frac{1}{m} \sum_{k=1}^m (\nabla l^k - \nabla\hat{\mathcal{L}})(\nabla l^k - \nabla\hat{\mathcal{L}})^\top \right] s \\ &= \sum_{i,j=1}^D s_i s_j \frac{1}{m-1} \frac{1}{m} \sum_{k=1}^m (\nabla l_i^k - \nabla\hat{\mathcal{L}}_i) (\nabla l_j^k - \nabla\hat{\mathcal{L}}_j) \\ &= \frac{1}{m-1} \sum_{i,j=1}^D s_i s_j \left(\frac{1}{m} \sum_{k=1}^m \nabla l_i^k \nabla l_j^k - \nabla\hat{\mathcal{L}}_i \nabla\hat{\mathcal{L}}_j - \nabla\hat{\mathcal{L}}_j \nabla\hat{\mathcal{L}}_i + \nabla\hat{\mathcal{L}}_i \nabla\hat{\mathcal{L}}_j \right) \\ &= \frac{1}{m-1} \left(\frac{1}{m} \sum_{k=1}^m \sum_{i,j=1}^D s_i \nabla l_i^k s_j \nabla l_j^k - \sum_{i,j=1}^D s_j \nabla\hat{\mathcal{L}}_j s_i \nabla\hat{\mathcal{L}}_i \right) \\ &= \frac{1}{m-1} \left(\frac{1}{m} \sum_{k=1}^m (s' \cdot \nabla l^k)^2 - (s' \cdot \nabla\hat{\mathcal{L}})^2 \right) \\ &= \frac{1}{m-1} \left(\frac{1}{m} \sum_{k=1}^m (s' \cdot \nabla l^k)^2 - \left(\frac{1}{m} \sum_{k=1}^m (s' \cdot \nabla l^k) \right)^2 \right).\end{aligned}\tag{22}$$

Comparing to $\sigma_{f'}$ yields

$$\begin{aligned}
 \eta_{f'} &= \frac{1}{m-1} \sum_{i,j=1}^D s_i s_j \left(\frac{1}{m} \sum_{k=1}^m \nabla l_i^k \nabla l_j^k - \nabla \hat{\mathcal{L}}_j \nabla \hat{\mathcal{L}}_i \right) \\
 &= \frac{1}{m-1} \sum_{i=1}^D s_i^2 \left(\frac{1}{m} \sum_{k=1}^m (\nabla l_i^k)^2 - \nabla \hat{\mathcal{L}}_i^2 \right) \\
 &\quad + \frac{1}{m-1} \sum_{i \neq j=1}^D s_i s_j \left(\frac{1}{m} \sum_{k=1}^m \nabla l_i^k \nabla l_j^k - \nabla \hat{\mathcal{L}}_j \nabla \hat{\mathcal{L}}_i \right) \\
 \eta_{f'} &= \sigma_{f'} + \frac{1}{m-1} \sum_{i \neq j=1}^D s_i s_j \left(\frac{1}{m} \sum_{k=1}^m \nabla l_i^k \nabla l_j^k - \nabla \hat{\mathcal{L}}_j \nabla \hat{\mathcal{L}}_i \right).
 \end{aligned} \tag{23}$$

From Eq (22) we see that in order to effectively compute $\eta_{f'}$ we need an efficient way of computing the inner product $(s(x)' \cdot \nabla l^k)$ for all k . In addition we need to know the search direction $s(x)$ of the potential next step (if x was accepted) at the time of computing $\eta_{f'}$. This is possible e.g. for the SGD search direction where $s(x) = -\frac{1}{m} \sum_{k=1}^m \nabla l^k(x)$ but potentially not possible or practical for arbitrary search directions. For all experiments in this paper we used the variance estimator $\sigma_{f'}$.

Appendix B. – Noise Sensitivity

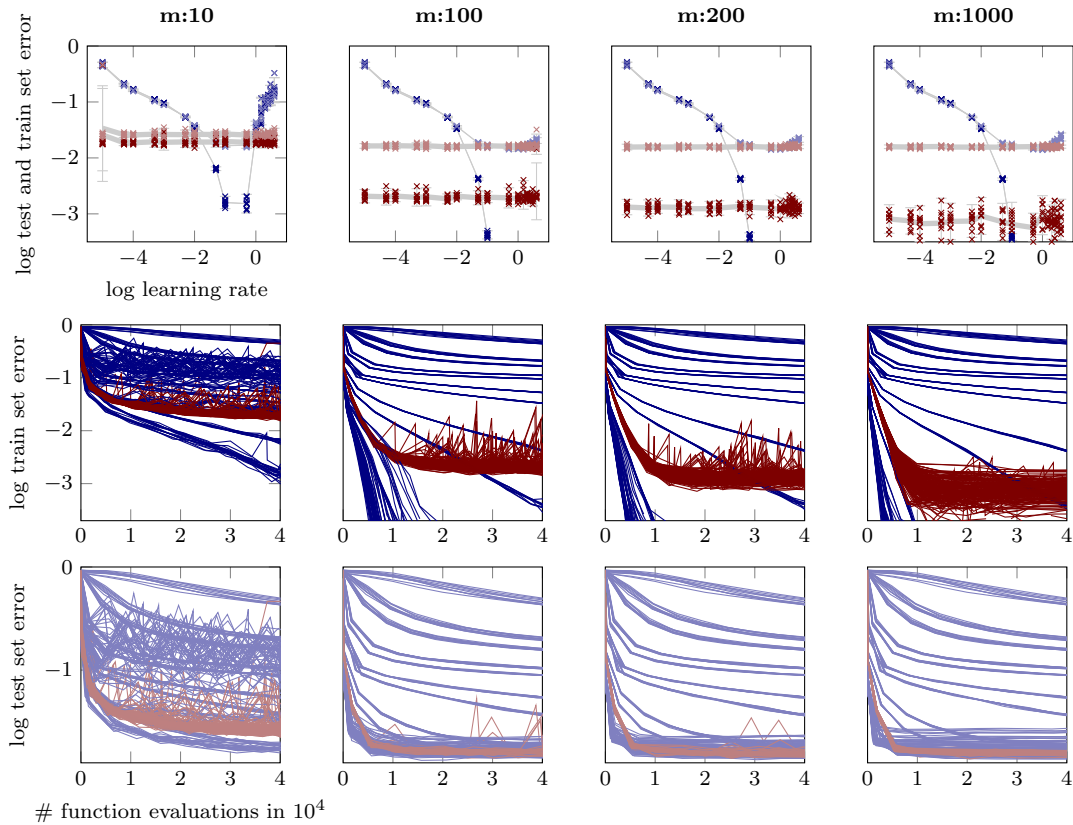


Figure 12: Performance of N-I on MNIST for *varying mini-batch sizes*. Plots and colors same as in Figure 6. Again the performance of SGD-runs with a fixed step size are very sensitive to its choice while SGD using the probabilistic line search are not. In this more shallow architecture SGD+problS performs well for all mini-batch sizes m . Except for $m = 10$ (Appendix A), *all* instances of SGD using the probabilistic line search reach the same *best* test set error. Similarly a good train set error is reached very fast by SGD+PROBLS (middle plots cropped for readability), though not the best one globally (as mentioned this advantage usually does not compromise a good test set error).

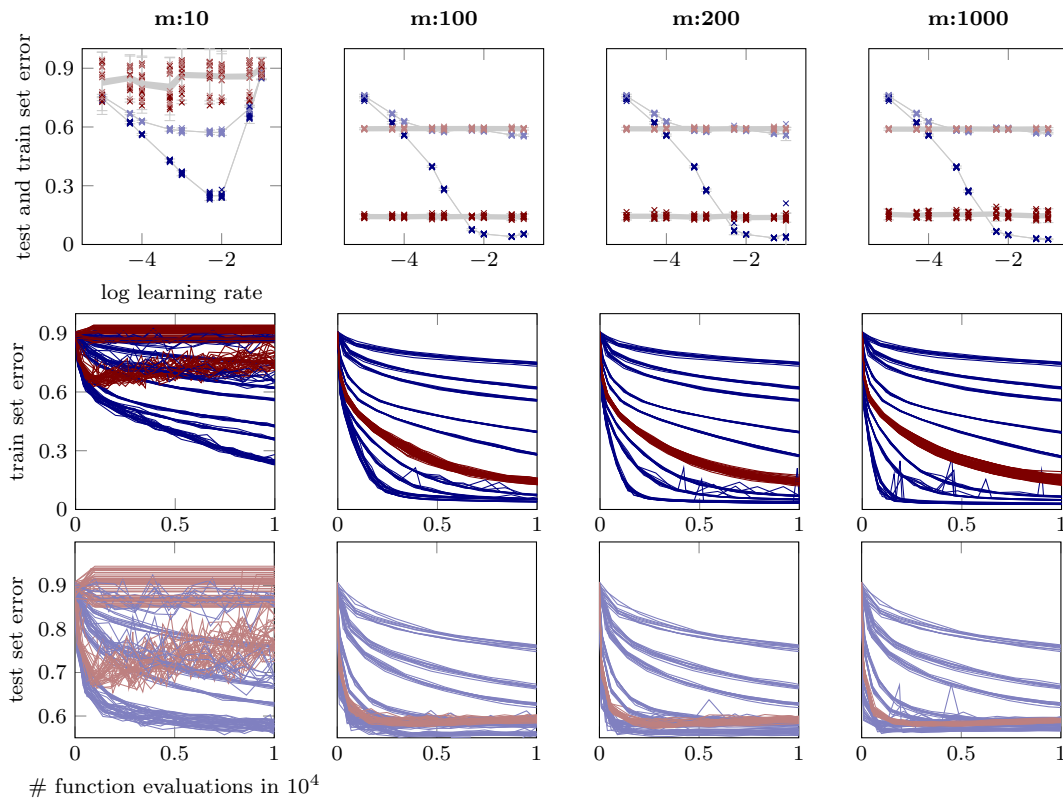


Figure 13: Performance of N-II on CIFAR-10 for *varying mini-batch sizes*. Plots and colors same as in Figure 6, except the scaling of the y-axis which is not logarithmic here. The experiments show the same results as for MNIST on this architecture. As expected, the performance of SGD-runs with a fixed step size are very sensitive to its choice while SGD-runs using the probabilistic line search are not. SGD+PROBLS performs well for all mini-batch sizes m . Except for $m = 10$, where the variance estimator becomes slightly brittle (Appendix A), *all* instances of SGD using the probabilistic line search reach best or close to best test set errors. Similarly a good train set error is reached very fast by SGD+PROBLS.

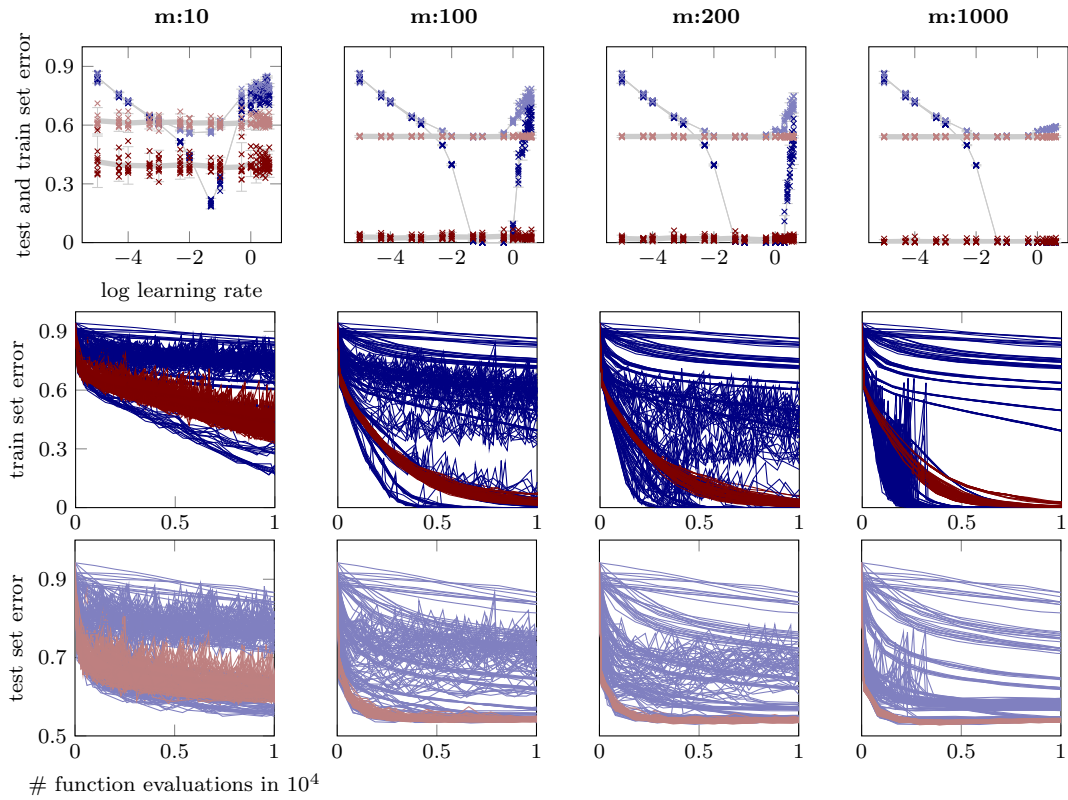


Figure 14: Performance of N-I on CIFAR-10 for *varying mini-batch sizes*. Plots and colors same as in Figure 13. Again the performance of SGD-runs with a fixed step size are very sensitive to its choice while SGD using the probabilistic line search are not. In this more shallow architecture SGD+PROBLS performs well for all mini-batch sizes m . Except for $m = 10$ (Appendix A), *all* instances of SGD using the probabilistic line search reach the same best test set error. Similarly a good train set error is reached very fast by SGD+PROBLS.

Appendix C. – Parameter Sensitivity

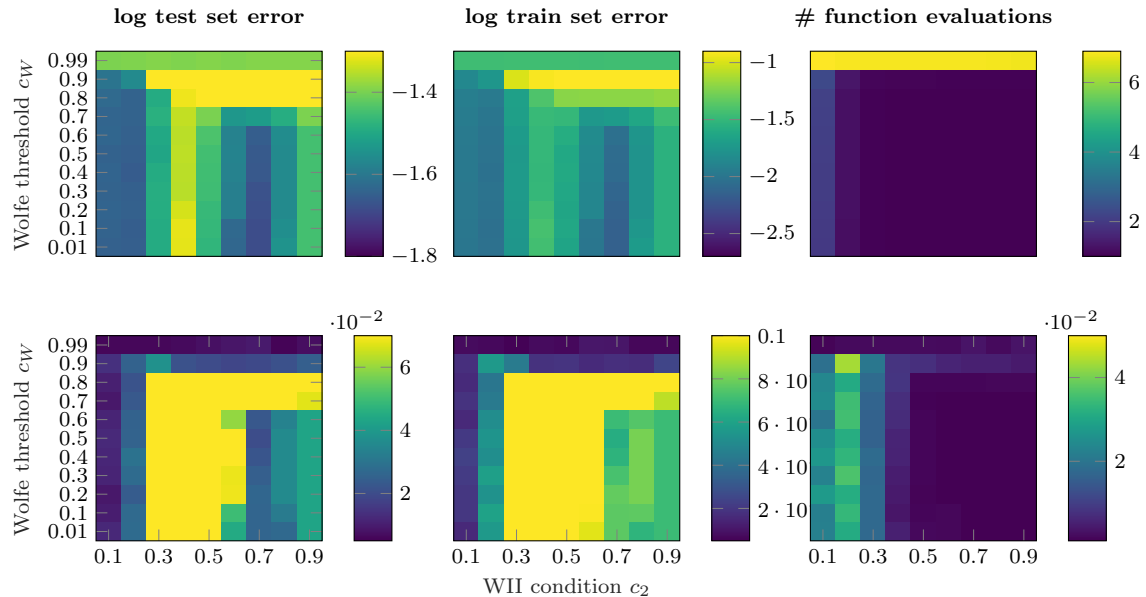


Figure 15: *Sensitivity to varying hyper parameters c_2 , and c_W and fixed $\alpha_{\text{ext}} = 1.0$ (§3.4).* Experimental setup as in Figures 8 and 9. Top row from left to right: logarithmic test set error, train set error, and average number of function evaluations per line search averaged over 10 different initializations. Bottom row: corresponding relative standard deviations. In all plots darker colors are better. For extrapolation parameters $\alpha_{\text{ext}} > 1$ (see Figures 16, 17, 18, and 19) the different parameter combinations all result in similar good performance. Only at extreme choices, for example $\alpha_{\text{ext}} = 1.0$ (this figure), which amounts to no extrapolation at all in between successive line searches, the line search becomes unstable. At the extreme value of $c_W = 0.99$, which amounts to imposing nearly absolute certainty about the Wolfe conditions, the line search becomes less efficient, though still does not break. In Figure 18 the default values adopted in the line search implementation ($c_W = 0.3$, $c_2 = 0.5$, and $\alpha_{\text{ext}} = 1.3$) are indicated as red dots.

PROBABILISTIC LINE SEARCHES

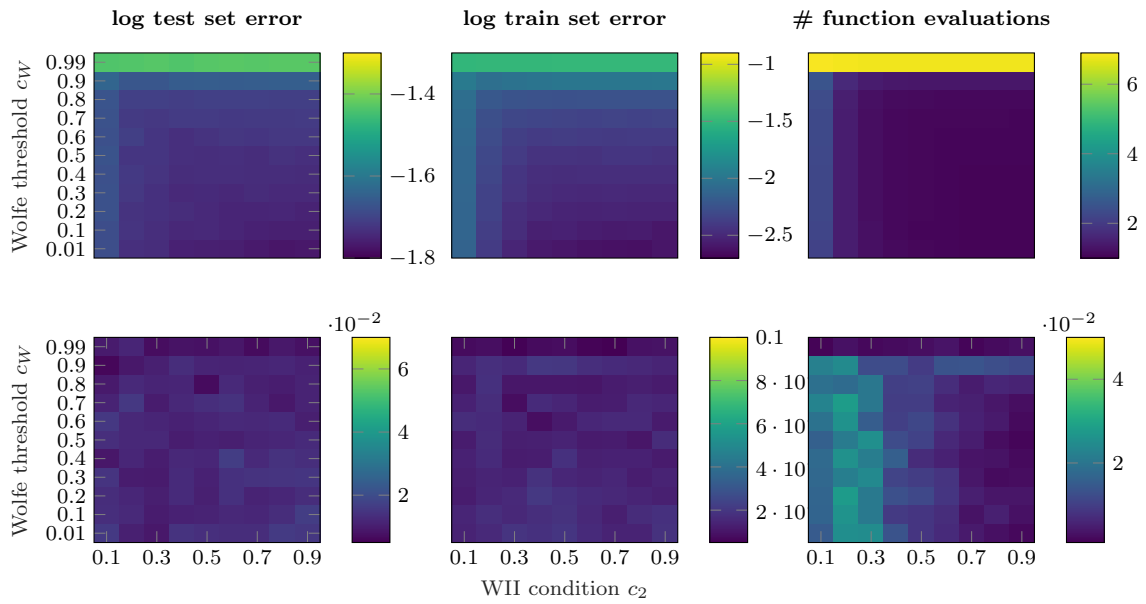


Figure 16: Same as Figure 15 but for *fixed* $\alpha_{\text{ext}} = 1.1$

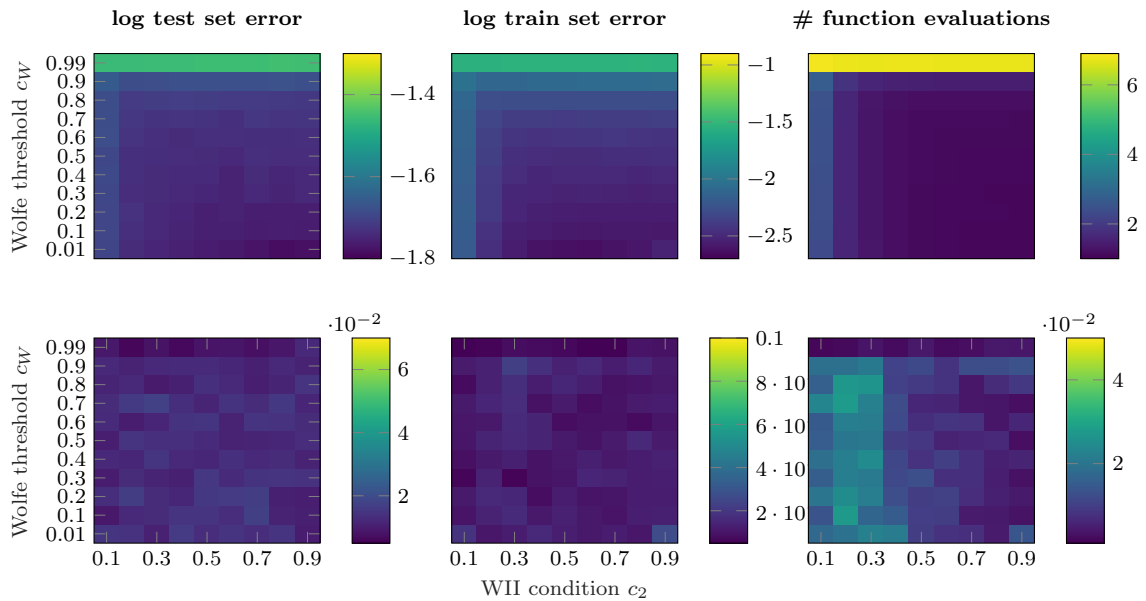


Figure 17: Same as Figure 15 but for *fixed* $\alpha_{\text{ext}} = 1.2$

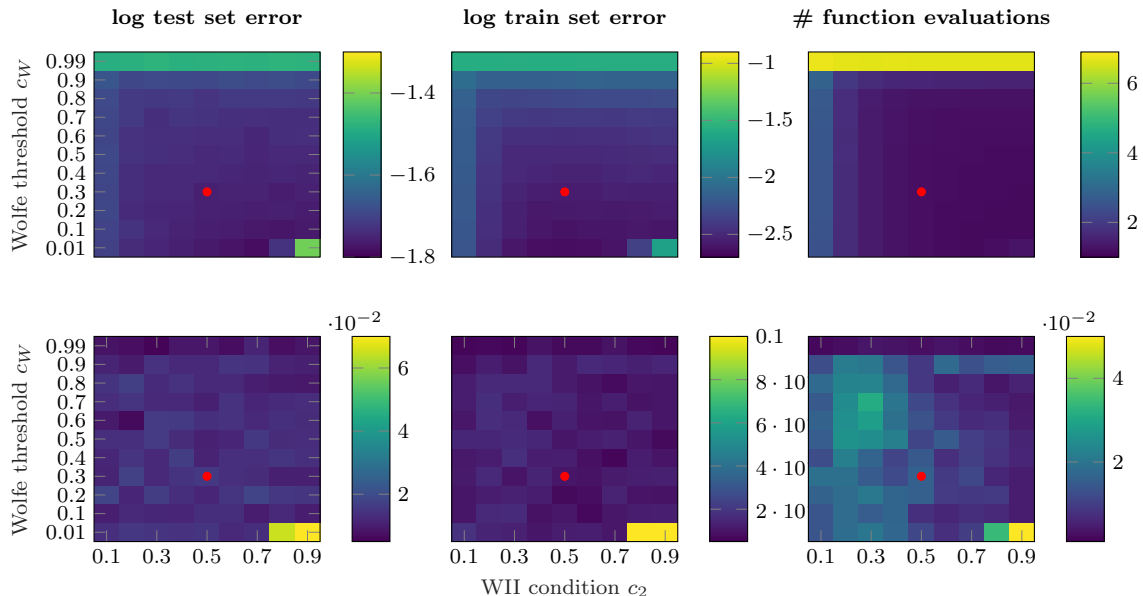


Figure 18: Same as Figure 15 but for *fixed* $\alpha_{\text{ext}} = 1.3$. The default values adopted in the line search implementation ($c_W = 0.3$, $c_2 = 0.5$, and $\alpha_{\text{ext}} = 1.3$) are indicated as red dots.

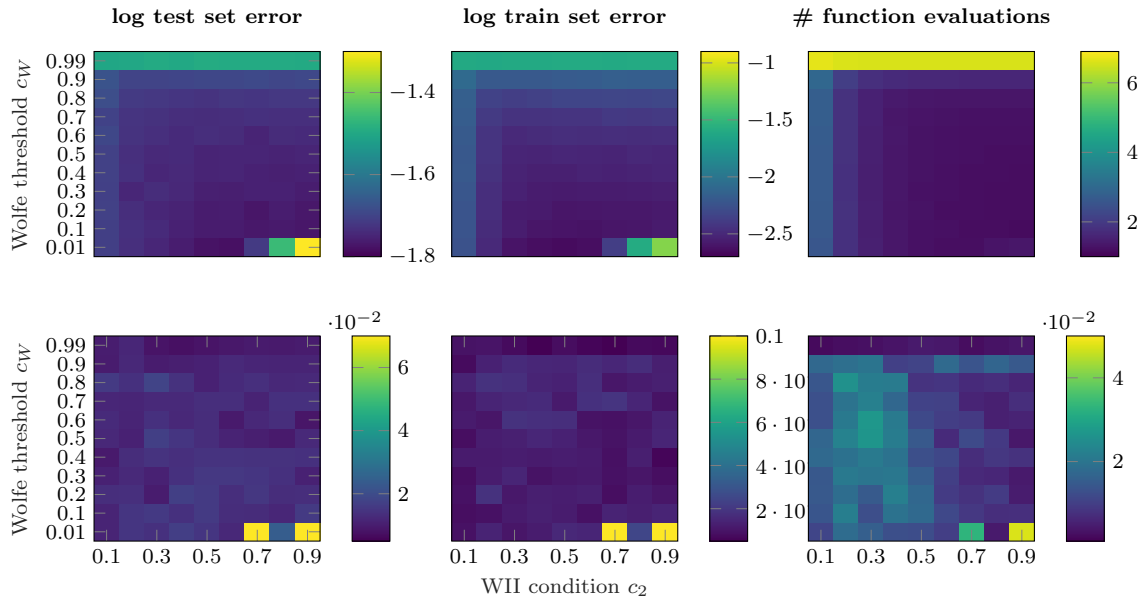


Figure 19: Same as Figure 15 but for *fixed* $\alpha_{\text{ext}} = 1.4$

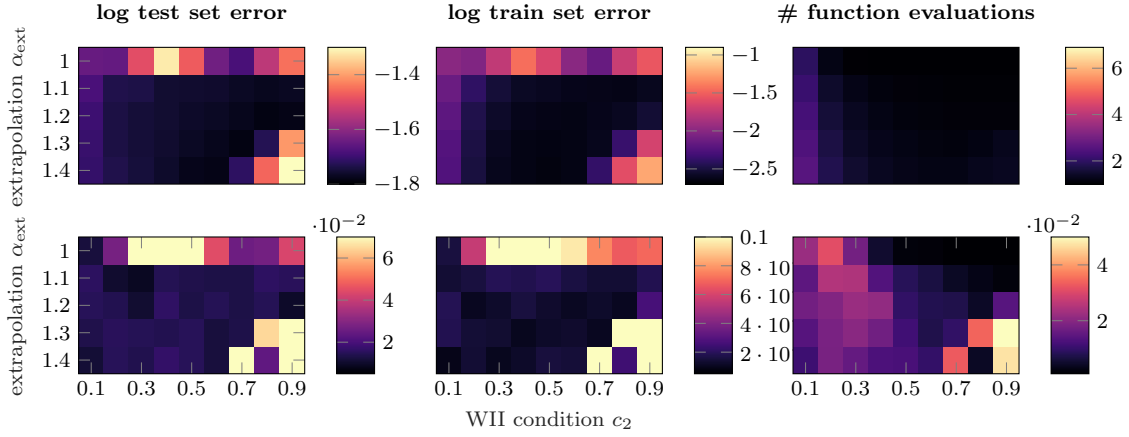


Figure 20: *Sensitivity to varying hyper parameters c_2 , and α_{ext} and fixed $c_W = 0.01$ (§3.4).* Experimental setup as in Figures 8 and 9 and plots like in Figure 15. In all plots darker colors are better. All choices of c_W result in good performance though very tight choices of $c_W = 0.99$ (Figure 30), which amounts to imposing nearly absolute certainty about the Wolfe conditions, are less efficient. As described by Figure 15, dropping the extrapolation factor $\alpha_{\text{ext}} \rightarrow 1$ in combination with a loose curvature condition (large c_2) renders the line search to break (top row, right half of columns in Figures 20–29). In Figure 25 the default values adopted in the line search implementation ($c_W = 0.3$, $c_2 = 0.5$, and $\alpha_{\text{ext}} = 1.3$) are indicated as red dots.

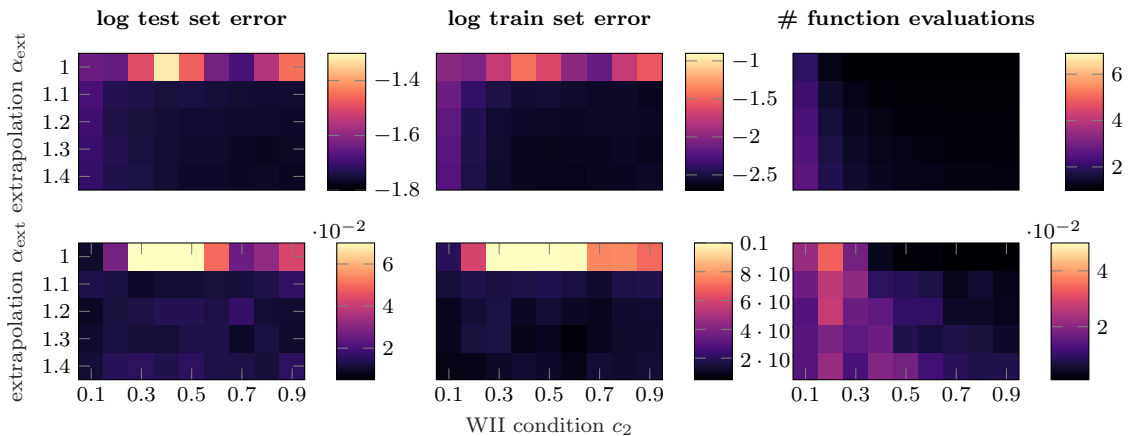


Figure 21: Same as Figure 20 but for *fixed $c_W = 0.10$.*

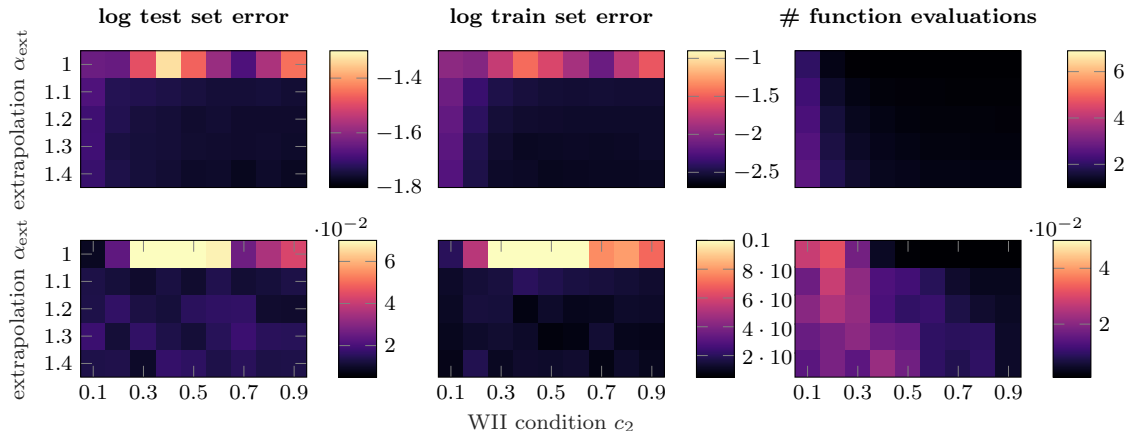


Figure 22: Same as Figure 20 but for *fixed* $c_W = 0.20$.

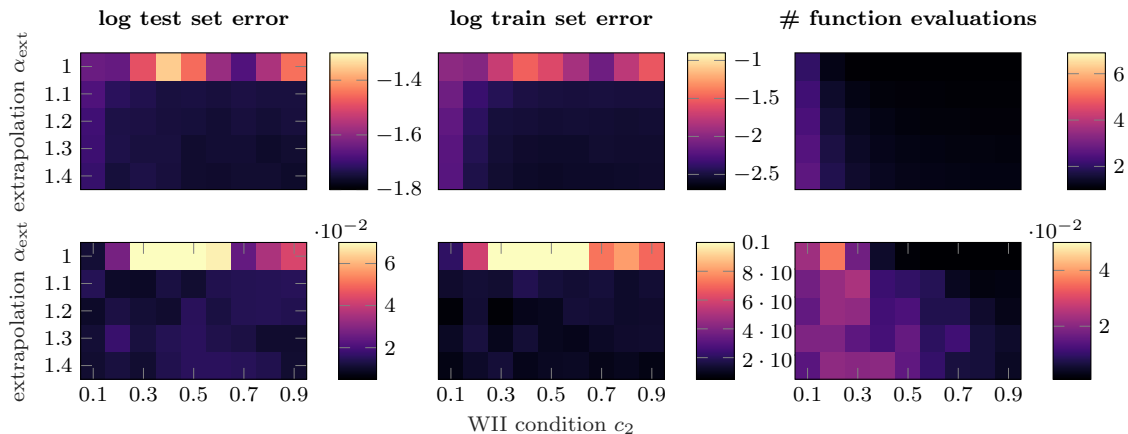


Figure 23: Same as Figure 20 but for *fixed* $c_W = 0.30$.

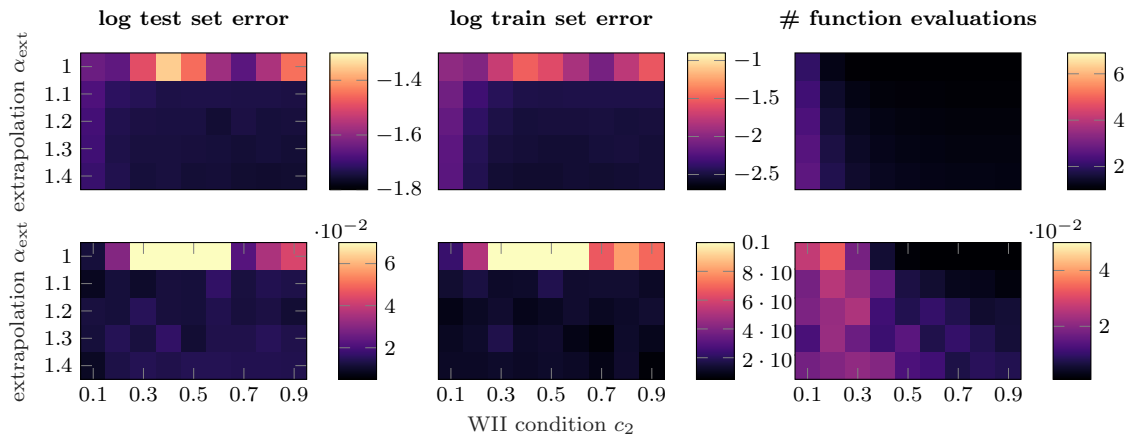


Figure 24: Same as Figure 20 but for *fixed* $c_W = 0.40$.

PROBABILISTIC LINE SEARCHES

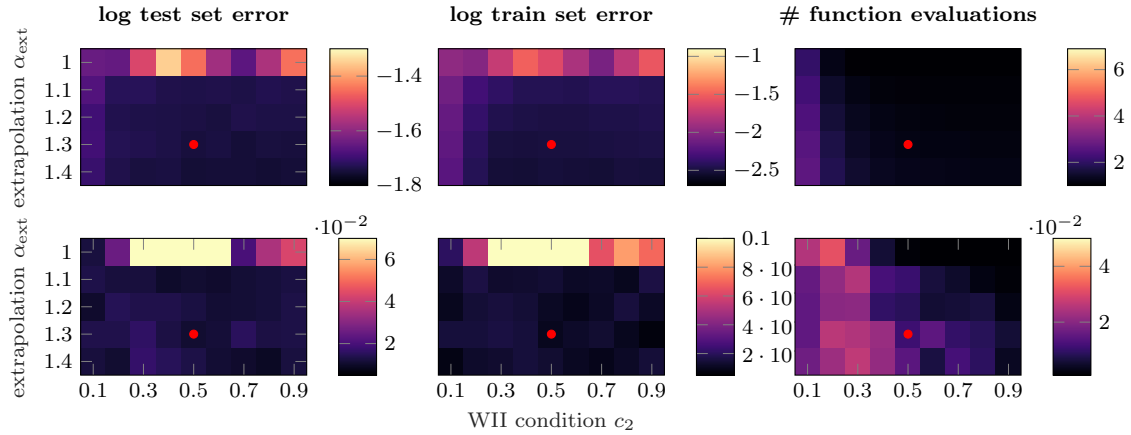


Figure 25: Same as Figure 20 but for *fixed* $c_W = 0.50$. The default values as red dots.

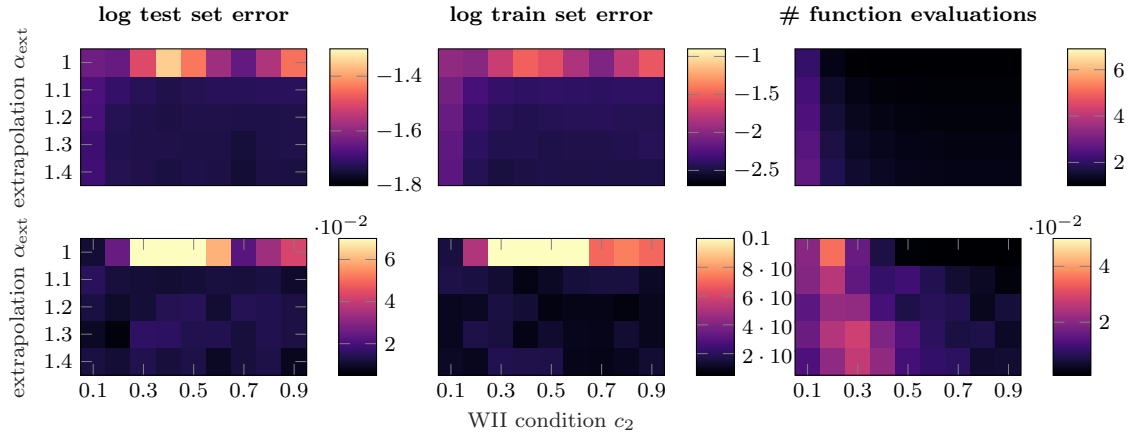


Figure 26: Same as Figure 20 but for *fixed* $c_W = 0.60$.

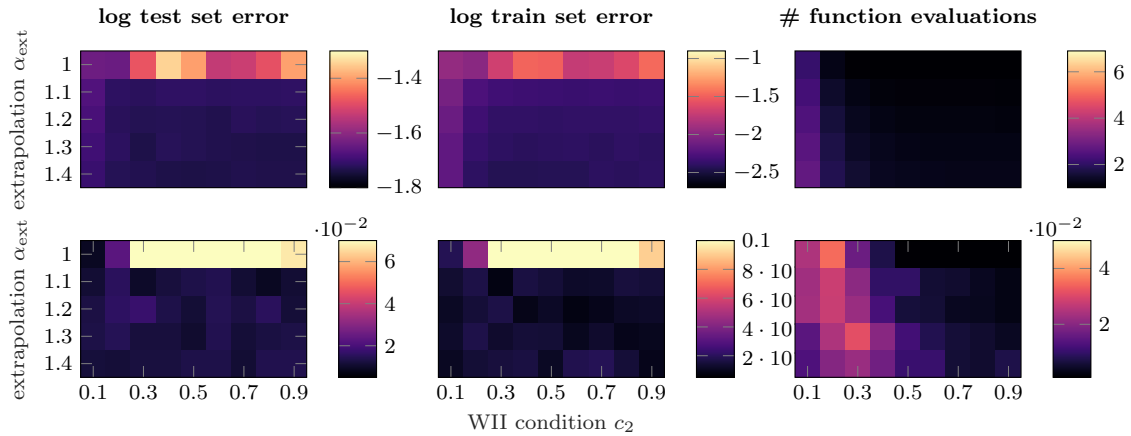


Figure 27: Same as Figure 20 but for *fixed* $c_W = 0.70$.

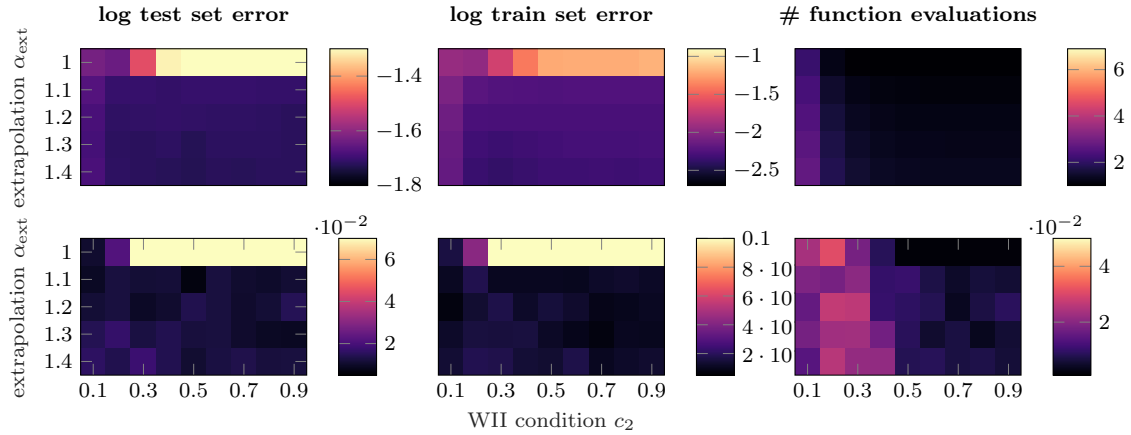


Figure 28: Same as Figure 20 but for *fixed* $c_W = 0.80$.

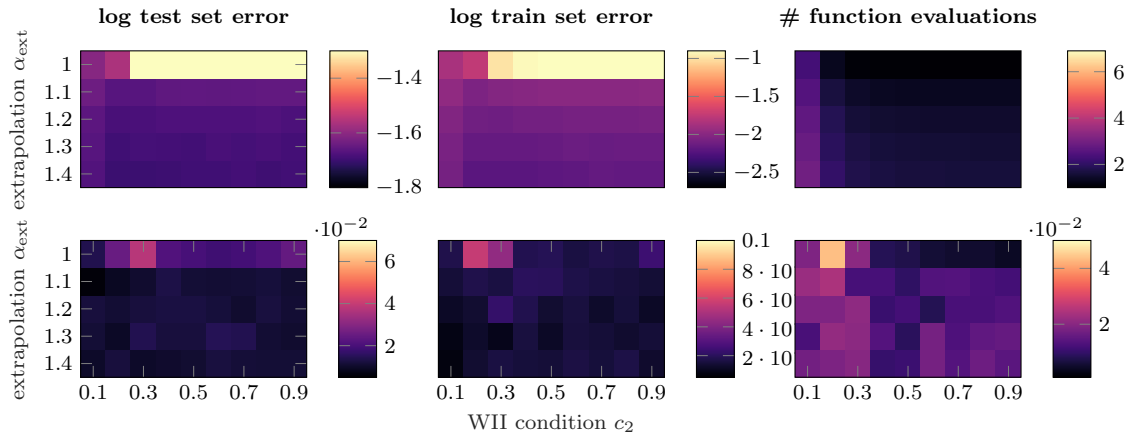


Figure 29: Same as Figure 20 but for *fixed* $c_W = 0.90$.

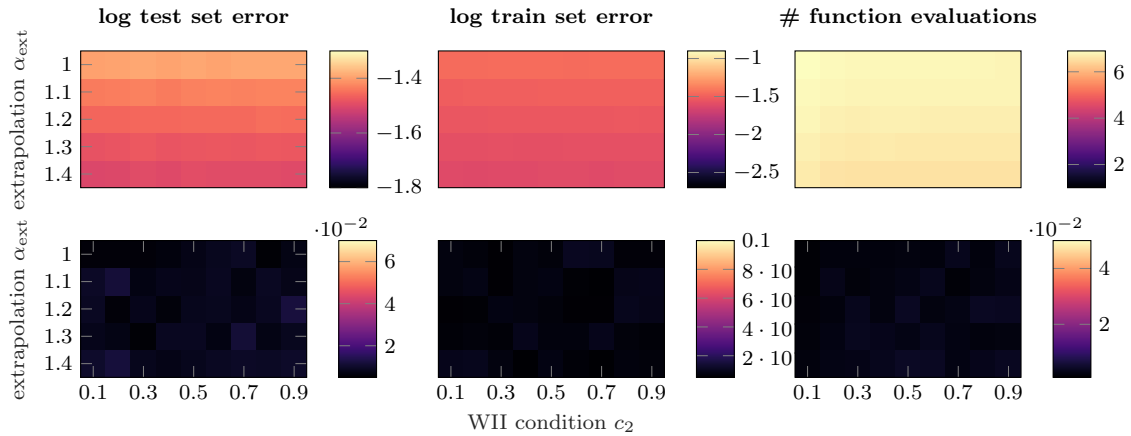


Figure 30: Same as Figure 20 but for *fixed* $c_W = 0.99$.

Appendix D. – Pseudocode

Algorithm 1 of Section 3 roughly sketches the structure of the probabilistic line search and its main ingredients. In this section we provide a detailed pseudocode. It is based on the code which was used for the experiments in this paper. A matlab implementation including a minimal example can be found at <http://tinyurl.com/probLineSearch>. The actual line search routine is called `PROBLINESEARCH` below and is quite short. Most of the pseudocode is occupied with comments, helper function that define the kernel of the GP, the GP-update or Gauss cdf and pdf which we printed here for completeness such that a detailed re-implementation is possible. For better readability of the pseudocode we use the following color coding:

- **blue**: comments
- **green**: variables of the integrated Wiener process.
- **red**: most recently evaluated observation (noisy loss and gradient). If the line search terminates, these will be returned as ‘accepted’.
- **orange**: inputs from the main solver procedure and unchanged during each line search.

Notation and operators:

operator or function	definition
$A \odot B$	elementwise multiplication
$A \oslash B$	elementwise division
$A.^b$	elementwise power of b
A'	transpose of A
A/B	right matrix division, the same as $A \cdot B^{-1}$
$A \setminus B$	left matrix division, the same as $A^{-1} \cdot B$
$A \cdot B$	scalar-scalar, scalar-matrix or matrix-matrix multiplication
$\text{sign}(a)$	sign of scalar a
$\text{erf}(x)$	error function $\text{erf}(x) = \frac{2}{\sqrt{\pi}} \int_0^x e^{-t^2} dt$
$\text{max}(A)$	maximum element in A
$\text{min}(A)$	minimum element in A
$ a $	absolute value of scalar
$A < B$	elementwise ‘less’ comparison
$A \leq B$	elementwise ‘less or equal’ comparison
$A > B$	elementwise ‘greater’ comparison
$A \geq B$	elementwise ‘greater or equal’ comparison
$[a, b, c] \leftarrow f(x)$	function f called at x returns the values a, b and c

For better readability we denote derivatives for example as dy and df (instead of y' and f' as in the main text).

```

1: function SGDSOLVER( $f$ )
2:     ▶  $f$  – function handle to objective. Usage:  $[y, dy, \Sigma_f, \Sigma_{df}] \leftarrow f(x)$ .
3:
4:     ▶ initial weights
5:      $x \leftarrow$  initial weights
6:
7:     ▶ initial step size and GP scale
8:      $\alpha \leftarrow e.g. \approx 10^{-4}$ 
9:      $\alpha_{stats} \leftarrow \alpha$ 
10:
11:    ▶ initial function evaluation at  $x$ 
12:     $[y, dy, \Sigma_f, \Sigma_{df}] \leftarrow f(x)$ 
13:
14:    ▶ initial search direction
15:     $d \leftarrow -dy$ 
16:
17:    ▶ loop over line searches
18:    while budget not used do
19:
20:        ▶ line search finds step size
21:         $[\alpha, \alpha_{stats}, x, y, dy, \Sigma_f, \Sigma_{df}] \leftarrow \text{PROBLINESEARCH}(x, d, y, dy, \Sigma_f, \Sigma_{df}, \alpha, \alpha_{stats}, f)$ 
22:
23:        ▶ set new search direction
24:         $d \leftarrow -dy$ 
25:    end while
26:
27:    return  $x$ 
28: end function

```

```

1: function PROBLINESEARCH( $x_0, d, f_0, df_0, \Sigma_{f_0}, \Sigma_{df_0}, \alpha_0, \alpha_{stats}, f$ )
2:     ▶  $x_0$  – current weights  $[D \times 1]$ 
3:     ▶  $f$  – function handle to objective.
4:     ▶
5:     ▶  $d$  – search direction  $[D \times 1]$  (does not need to be normalized)
6:     ▶  $f_0$  – function value at start,  $f_0 = f(x_0)$ 
7:     ▶  $df_0$  – gradient at start,  $df_0 = \nabla f(x_0)$   $[D \times 1]$ 
8:     ▶  $\Sigma_{f_0}$  – sample variance of  $f_0$ 
9:     ▶  $\Sigma_{df_0}$  – sample variances of  $df_0$ ,  $[D \times 1]$ 
10:    ▶  $\alpha_0$  – initial step size
11:
12:    ▶ set maximum # of  $f$  evaluations per line search
13:     $L \leftarrow 6$ 

```

```

14:   ▶ scaling and noise level of GP
15:    $\beta \leftarrow |d' \cdot \Sigma_{df_0}|$  ▷ scale factor
16:    $\sigma_f \leftarrow \sqrt{\Sigma_{f_0} / (\alpha_0 \cdot \beta)}$  ▷ scaled sample variance of  $f_0$ 
17:    $\sigma_{df} \leftarrow \sqrt{((d \cdot 2)^T \cdot \Sigma_{df_0})} / \beta$  ▷ scaled and projected sample variances of  $df_0$ 
18:
19:   ▶ initialize counter and non-fixed parameters
20:    $N \leftarrow 1$  ▷ size of GP =  $2 \cdot N$ 
21:    $t_{ext} \leftarrow 1$  ▷ scaled step size for extrapolation
22:    $tt \leftarrow 1$  ▷ scaled position of first function evaluation
23:
24:   ▶ initialize storage for GP. Dynamic arrays of maximum size  $[L + 1 \times 1]$ 
25:    $T \leftarrow [0]$  ▷ scaled positions along search direction
26:    $Y \leftarrow [0]$  ▷ scaled function values at  $T$ 
27:    $dY_p \leftarrow [(df_0' \cdot d) / \beta]$  ▷ scaled projected gradients at  $T$ 
28:
29:   ▶ initialize GP with observation at start
30:    $[G, A] \leftarrow \text{UPDATEGP}(T, Y, dY_p, N, \sigma_f, \sigma_{df})$ 
31:
32:   ▶ loop until budget is used or acceptable point is found
33:   for  $N$  from 2 to  $L + 1$  do
34:
35:       ▶ evaluate objective function at  $tt$ .
36:        $[y, dy, \Sigma_f, \Sigma_{df}, T, Y, dY_p, N] \leftarrow \text{EVALUATEOBJECTIVE}(tt, x_0, \alpha_0, d, T, Y, dY_p, N, \beta, f)$ 
37:
38:       ▶ update the GP which is now of size  $2 \cdot N$ .
39:        $[G, A] \leftarrow \text{UPDATEGP}(T, Y, dY_p, N, \sigma_f, \sigma_{df})$ 
40:
41:       ▶ initialize storage for candidates. Dynamic arrays of maximum size  $[N \times 1]$ .
42:        $T_{cand} \leftarrow []$  ▷ scaled position of candidates
43:        $M_{cand} \leftarrow []$  ▷ GP mean of candidates
44:        $S_{cand} \leftarrow []$  ▷ GP standard deviation of candidates
45:
46:       ▶ current point is above the Wolfe threshold? If yes, accept point and return.
47:       if  $\text{PROBWOLFE}(tt, T, A, G)$  then
48:            $output \leftarrow \text{RESCALEOUTPUT}(x_0, f_0, \alpha_0, d, tt, y, dy, \Sigma_f, \Sigma_{df}, \beta)$ 
49:           return  $output$ 
50:       end if
51:
52:       ▶ Wolfe conditions not satisfied at this point.
53:       ▶ find suitable candidates for next evaluation.
54:
55:       ▶ GP mean of function values and corresponding gradients at points in  $T$ .
56:        $M \leftarrow \text{map function } M(-, T, A) \text{ over } T$ 
57:        $dM \leftarrow \text{map function } D1M(-, T, A) \text{ over } T$ 

```

```

58:     ▶ candidates 1: local minima of GP mean.
59:      $T_{sorted} \leftarrow$  sort  $T$  in ascending order
60:      $T_{Wolfes} \leftarrow [ ]$                                      ▷ prepare list of acceptable points
61:
62:     ▶ iterate through all  $N - 1$  cells, compute locations of local minima.
63:     for  $n$  from 1 to  $N - 1$  do
64:          $T_n \leftarrow$  value of  $T_{sorted}$  at  $n$ 
65:          $T_{n+1} \leftarrow$  value of  $T_{sorted}$  at  $n + 1$ 
66:
67:         ▶ add a little offset for numerical stability
68:          $t_{rep} \leftarrow T_n + 1^{-6} \cdot (T_{n+1} - T_n)$ 
69:
70:         ▶ compute location of cubic minimum in  $n^{\text{th}}$  cell
71:          $t_{cubMin} \leftarrow$  CUBICMINIMUM( $t_{rep}, T, A, N$ )
72:
73:         ▶ add point to candidate list if minimum lies in between  $T_n$  and  $T_{n+1}$ 
74:         if  $t_{cubMin} > T_n$  and  $t_{cubMin} < T_{n+1}$  then
75:             if (not isnanOrIsinf( $t_{cubMin}$ )) and ( $t_{cubMin} > 0$ ) then
76:                  $T_{cand} \leftarrow$  append  $t_{cubMin}$ 
77:                  $M_{cand} \leftarrow$  append  $M(t_{cubMin}, T, A)$ 
78:                  $S_{cand} \leftarrow$  append  $V(t_{cubMin}, T, G)$ 
79:             end if
80:         else
81:
82:             ▶ most likely uphill? If yes, break.
83:             if  $n = 1$  and  $D1M(0, T, A) > 0$  then
84:                  $r \leftarrow 0.01$ 
85:                  $tt \leftarrow r \cdot (T_n + T_{n+1})$ 
86:
87:                 ▶ evaluate objective function at  $tt$  and return.
88:                  $[y, dy, \Sigma_f, \Sigma_{df}, T, Y, dY_p, N] \leftarrow$  EVALUATEOBJECTIVE( $tt, x_0, \alpha_0, d, T, Y, dY_p, N, \beta, f$ )
89:
90:                  $output \leftarrow$  RESCALEOUTPUT( $x_0, f_0, \alpha_0, d, tt, y, dy, \Sigma_f, \Sigma_{df}, \beta$ )
91:                 return  $output$ 
92:             end if
93:         end if
94:
95:         ▶ check whether there is an acceptable point among the old evaluations
96:         if  $n > 1$  and  $PROBWOLFE(T_n, T, A, G)$  then
97:              $T_{Wolfes} \leftarrow$  append  $T_n$ 
98:         end if
99:     end for
100:
101:     ▶ check if acceptable points exists and return
102:     if  $T_{Wolfes}$  is not empty then
    
```

```

103:     ▶ if last evaluated point is among acceptable ones, return it.
104:     if  $tt$  in  $T_{Wolfes}$  then
105:          $output \leftarrow \text{RESCALEOUTPUT}(x_0, f_0, \alpha_0, d, tt, y, dy, \Sigma_f, \Sigma_{df}, \beta)$ 
106:         return  $output$ 
107:     end if
108:
109:     ▶ else, choose the one with the lowest GP mean and re-evaluate its gradient.
110:      $M_{Wolfes} \leftarrow \text{map } M(-, T, A) \text{ over } T_{Wolfes}$ 
111:      $tt \leftarrow \text{value of } T_{Wolfes} \text{ at index of } \min(M_{Wolfes})$ 
112:
113:     ▶ evaluate objective function at  $tt$ .
114:      $[y, dy, \Sigma_f, \Sigma_{df}, T, Y, dY_p, N] \leftarrow \text{EVALUATEOBJECTIVE}(tt, x_0, \alpha_0, d, T, Y, dY_p, N, \beta, f)$ 
115:
116:      $output \leftarrow \text{RESCALEOUTPUT}(x_0, f_0, \alpha_0, d, tt, y, dy, \Sigma_f, \Sigma_{df}, \beta)$ 
117:     return  $output$ 
118: end if
119:
120: ▶ candidates 2: one extrapolation step
121:  $T_{cand} \leftarrow \text{append } \max(T) + t_{ext}$ 
122:  $M_{cand} \leftarrow \text{append } M(\max(T) + t_{ext}, T, A)$ 
123:  $S_{cand} \leftarrow \text{append } V(\max(T) + t_{ext}, T, G)^{\frac{1}{2}}$ 
124:
125: ▶ find minimal mean among  $M$ .
126:  $\mu_{EI} \leftarrow \text{minimal value of } M$ 
127:
128: ▶ compute expected improvement and Wolfe probabilities at  $T_{cand}$ 
129:  $EI_{cand} \leftarrow \text{EXPECTEDIMPROVEMENT}(M_{cand}, S_{cand}, \mu_{EI})$ 
130:  $PP_{cand} \leftarrow \text{map } \text{PROBWOLFE}(-, T, A, G) \text{ over } T_{cand}$ 
131:
132: ▶ choose point among candidates that maximizes  $EI_{cand} \wedge PP_{cand}$ 
133:  $i_{bestCand} \leftarrow \text{index of } \max(EI_{cand} \odot PP_{cand})$ 
134:  $tt_{bestCand} \leftarrow \text{value of } T_{cand} \text{ at } i_{bestCand}$ 
135:
136: ▶ extend extrapolation step if necessary
137: if  $tt_{bestCand}$  is equal to  $tt + t_{ext}$  then
138:      $t_{ext} \leftarrow 2 \cdot t_{ext}$ 
139: end if
140:
141: ▶ set location for next evaluation
142:  $tt \leftarrow tt_{bestCand}$ 
143: end for
144:
145: ▶ limit reached: evaluate a final time and return the point with lowest GP mean
146:  $[y, dy, \Sigma_f, \Sigma_{df}, T, Y, dY_p, N] \leftarrow \text{EVALUATEOBJECTIVE}(tt, x_0, \alpha_0, d, T, Y, dY_p, N, \beta, f)$ 

```

```

147:   ▶ update the GP which is now of size  $2 \cdot N$ .
148:    $[G, A] \leftarrow \text{UPDATEGP}(T, Y, dY_p, N, \sigma_f, \sigma_{df})$ 
149:
150:   ▶ check last point for acceptance
151:   if  $\text{PROBWOLFE}(tt, T, A, G)$  then
152:        $output \leftarrow \text{RESCALEOUTPUT}(x_0, f_0, \alpha_0, d, tt, y, dy, \Sigma_f, \Sigma_{df}, \beta)$ 
153:       return  $output$ 
154:   end if
155:
156:   ▶ at the end of budget return point with the lowest GP mean
157:   ▶ compute GP means at  $T$ 
158:    $M \leftarrow \text{map } M(-, T, A)$  over  $T$ 
159:    $i_{lowest} \leftarrow$  index of minimal value in  $M$ 
160:    $t_{lowest} \leftarrow$  value of  $T$  at  $i_{lowest}$ 
161:
162:   ▶ if  $t_{lowest}$  is the last evaluated point, return
163:   if  $t_{lowest}$  is equal to  $tt$  then
164:        $output \leftarrow \text{RESCALEOUTPUT}(x_0, f_0, \alpha_0, d, tt, y, dy, \Sigma_f, \Sigma_{df}, \beta)$ 
165:       return  $output$ 
166:   end if
167:
168:   ▶ else, re-evaluate its gradient and return
169:    $tt \leftarrow$  value of  $t_{lowest}$ 
170:
171:   ▶ evaluate objective function at  $tt$ .
172:    $[y, dy, \Sigma_f, \Sigma_{df}, T, Y, dY_p, N] \leftarrow \text{EVALUATEOBJECTIVE}(tt, x_0, \alpha_0, d, T, Y, dY_p, N, \beta, f)$ 
173:
174:    $output \leftarrow \text{RESCALEOUTPUT}(x_0, f_0, \alpha_0, d, tt, y, dy, \Sigma_f, \Sigma_{df}, \beta)$ 
175:   return  $output$ 
176: end function

```

```

1: function  $\text{RESCALEOUTPUT}(x_0, f_0, \alpha_0, d, tt, y, dy, \Sigma_f, \Sigma_{df}, \beta, \alpha_{stats})$ 
2:   ▶ design parameters
3:    $\alpha_{ext} \leftarrow 1.3$  ▷ extrapolation parameter
4:    $\theta_{reset} \leftarrow 100$  ▷ reset threshold for GP scale
5:
6:   ▶ rescale accepted step size
7:    $\alpha_{acc} \leftarrow tt \cdot \alpha_0$ 
8:
9:   ▶ update weights
10:   $x_{acc} \leftarrow x_0 + \alpha_{acc} \cdot d$ 
11:
12:  ▶ rescale accepted function value
13:   $f_{acc} \leftarrow y \cdot (\alpha_0 \cdot \beta) + f_0$ 

```

```

14:   ▶ accepted gradient
15:    $df_{acc} \leftarrow dy$ 
16:
17:   ▶ sample variance of  $f_{acc}$ 
18:    $\Sigma_{f_{acc}} \leftarrow \Sigma_f$ 
19:
20:   ▶ sample variances of  $df_{acc}$ 
21:    $\Sigma_{df_{acc}} \leftarrow \Sigma_{df}$ 
22:
23:   ▶ update exponential running average of scalings
24:    $\gamma \leftarrow 0.95$ 
25:    $\alpha_{stats} \leftarrow \gamma \cdot \alpha_{stats} + (1 - \gamma) \cdot \alpha_{acc}$ 
26:
27:   ▶ next initial step size
28:    $\alpha_{next} \leftarrow \alpha_{acc} \cdot \alpha_{ext}$ 
29:
30:   ▶ if new GP scaling is drastically different than previous ones reset it.
31:   if ( $\alpha_{next} < \alpha_{stats}/\theta_{reset}$ ) or ( $\alpha_{next} > \alpha_{stats} \cdot \theta_{reset}$ ) then
32:      $\alpha_{next} \leftarrow \alpha_{stats}$ 
33:   end if
34:
35:   ▶ compressed output for readability of pseudocode
36:    $output \leftarrow [\alpha_{next}, \alpha_{stats}, x_{acc}, f_{acc}, df_{acc}, \Sigma_{f_{acc}}, \Sigma_{df_{acc}}]$ 
37:
38:   return  $output$ 
39: end function

```

```

1: function EVALUATEOBJECTIVE( $tt, x_0, \alpha_0, d, T, Y, dY_p, N, \beta, f$ )
2:   ▶ evaluate objective function at  $tt$ 
3:    $[y, dy, \Sigma_f, \Sigma_{df}] \leftarrow f(x_0 + tt \cdot \alpha_0 \cdot d)$ 
4:
5:   ▶ scale output
6:    $y \leftarrow (y - f_0)/(\alpha_0 \cdot \beta)$ 
7:    $dy_p \leftarrow (dy' \cdot d)/\beta$ 
8:
9:   ▶ storage
10:   $T \leftarrow$  append  $tt$ 
11:   $Y \leftarrow$  append  $y$ 
12:   $dY_p \leftarrow$  append  $dy_p$ 
13:   $N \leftarrow N + 1$ 
14:
15:  return  $[y, dy, \Sigma_f, \Sigma_{df}, T, Y, dY_p, N]$ 
16: end function

```

```

1: function CUBICMINIMUM( $t, T, A, N$ )
2:   ► compute necessary derivatives of GP mean at  $t$ 
3:    $d1m_t \leftarrow D1M(t, T, A)$ 
4:    $d2m_t \leftarrow D2M(t, T, A)$ 
5:    $d3m_t \leftarrow D3M(t, T, A, N)$ 
6:    $a \leftarrow 0.5 \cdot d3m_t$ 
7:    $b \leftarrow d2m_t - t \cdot d3m_t$ 
8:    $c \leftarrow d1m_t - d2m_t \cdot t + 0.5 \cdot d3m_t \cdot t^2$ 
9:
10:  ► third derivative is almost zero  $\rightarrow$  essentially a quadratic, single extremum
11:  if  $|d3m_t| < 1^{-9}$  then
12:     $t_{cubMin} \leftarrow -(d1m_t - t \cdot d2m_t)/d2m_t$ 
13:    return  $t_{cubMin}$ 
14:  end if
15:
16:  ► roots are complex, no extremum
17:   $\lambda \leftarrow b^2 - 4 \cdot a \cdot c$ 
18:  if  $\lambda < 0$  then
19:     $t_{cubMin} \leftarrow +\infty$ 
20:    return  $t_{cubMin}$ 
21:  end if
22:
23:  ► compute the two possible roots
24:   $LR \leftarrow (-b - \text{sign}(a) \cdot \sqrt{\lambda})/(2 \cdot a)$  ▷ left Root
25:   $RR \leftarrow (-b + \text{sign}(a) \cdot \sqrt{\lambda})/(2 \cdot a)$  ▷ right Root
26:
27:  ► calculate the two values of the cubic at those points (up to a constant)
28:   $dt_L \leftarrow LR - t$  ▷ distance to left root
29:   $dt_R \leftarrow RR - t$  ▷ distance to right root
30:   $CV_L \leftarrow d1m_t \cdot dt_L + 0.5 \cdot d2m_t \cdot dt_L^2 + (d3m_t \cdot dt_L^3)/6$  ▷ left cubic value
31:   $CV_R \leftarrow d1m_t \cdot dt_R + 0.5 \cdot d2m_t \cdot dt_R^2 + (d3m_t \cdot dt_R^3)/6$  ▷ right cubic value
32:
33:  ► find the minimum and return it.
34:  if  $CV_L < CV_R$  then
35:     $t_{cubMin} \leftarrow LR$ 
36:  else
37:     $t_{cubMin} \leftarrow RR$ 
38:  end if
39:
40:  return  $t_{cubMin}$ 
41:
42: end function

```

```

1: function UPDATEGP( $T, Y, dY_p, N, \sigma_f, \sigma_{df}$ )
2:   ► initialize kernel matrices
3:    $k_{TT} \leftarrow [N \times N]$  matrix with zeros           ▷ covariance of function values
4:    $kd_{TT} \leftarrow [N \times N]$  matrix with zeros     ▷ covariance of function values and gradients
5:    $dkd_{TT} \leftarrow [N \times N]$  matrix with zeros    ▷ covariance of gradients
6:
7:   ► fill kernel matrices
8:   for  $i = 1$  to  $N$  do
9:     for  $j = 1$  to  $N$  do
10:       $k_{TT}(i, j) \leftarrow \text{K}(T(i), T(j))$ 
11:       $kd_{TT}(i, j) \leftarrow \text{KD}(T(i), T(j))$ 
12:       $dkd_{TT}(i, j) \leftarrow \text{DKD}(T(i), T(j))$ 
13:     end for
14:   end for
15:
16:   ► build diagonal covariance matrix of Gaussian likelihood  $[2N \times 2N]$ .
17:    $\Lambda \leftarrow \begin{bmatrix} \text{diag}(\sigma_f^2)_{N \times N} & 0_{N \times N} \\ 0_{N \times N} & \text{diag}(\sigma_{df}^2)_{N \times N} \end{bmatrix}$ 
18:
19:    $G \leftarrow \begin{pmatrix} k_{TT} & kd_{TT} \\ kd'_{TT} & dkd_{TT} \end{pmatrix} + \Lambda$            ▷  $[2N \times 2N]$  matrix
20:
21:   ► residual between observed and predicted data
22:    $\Delta \leftarrow \begin{pmatrix} Y \\ dY_p \end{pmatrix}$            ▷  $[2N \times 1]$  vector
23:
24:   ► compute weighted observations  $A$ .
25:    $A \leftarrow G \backslash \Delta$            ▷  $[2N \times 1]$  vector
26:
27:   return  $[G, A]$ 
28:
29: end function

```

```

1: function M( $t, T, A$ )
2:     ► posterior mean at  $t$ 
3:     return [K( $t, T'$ ), KD( $t, T'$ )] ·  $A$ 
4: end function
5:
6: function D1M( $t, T, A$ )
7:     ► first derivative of mean at  $t$ 
8:     return [DK( $t, T'$ ), DKD( $t, T'$ )] ·  $A$ 
9: end function
10:
11: function D2M( $t, T, A$ )
12:     ► second derivative of mean at  $t$ 
13:     return [DDK( $t, T'$ ), DDKD( $t, T'$ )] ·  $A$ 
14: end function
15:
16: function D3M( $t, T, A, N$ )
17:     ► third derivative of mean at  $t$ 
18:     return [DDDK( $t, T'$ ), ZEROS(1, N)] ·  $A$ 
19: end function
20:
21: function V( $t, T, G$ )
22:     ► posterior variance of function values at  $t$ 
23:     return K( $t, t$ ) - [K( $t, T'$ ), KD( $t, T'$ )] · ( $G \setminus$  [K( $t, T'$ ), KD( $t, T'$ )]')
24: end function
25:
26: function VD( $t, T, G$ )
27:     ► posterior variance of function values and derivatives at  $t$ 
28:     return KD( $t, t$ ) - [K( $t, T'$ ), KD( $t, T'$ )] · ( $G \setminus$  [DK( $t, T'$ ), DKD( $t, T'$ )]')
29: end function
30:
31: function DVD( $t, T, G$ )
32:     ► posterior variance of derivatives at  $t$ 
33:     return DKD( $t, t$ ) - [DK( $t, T'$ ), DKD( $t, T'$ )] · ( $G \setminus$  [DK( $t, T'$ ), DKD( $t, T'$ )]')
34: end function
35:
36: function V0F( $t, T, G$ )
37:     ► posterior covariances of function values at  $t = 0$  and  $t$ 
38:     return K(0,  $t$ ) - [K(0,  $T'$ ), KD(0,  $T'$ )] · ( $G \setminus$  [K( $t, T'$ ), KD( $t, T'$ )]')
39: end function
40:
41: function VD0F( $t, T, G$ )
42:     ► posterior covariance of gradient and function value at  $t = 0$  and  $t$  respectively
43:     return DK(0,  $t$ ) - [DK(0,  $T'$ ), DKD(0,  $T'$ )] · ( $G \setminus$  [K( $t, T'$ ), KD( $t, T'$ )]')
44: end function

```

```

45: function V0DF( $t, T, G$ )
46:   ► posterior covariance of function value and gradient at  $t = 0$  and  $t$  respectively
47:   return  $\text{KD}(0, t) - [\text{K}(0, T'), \text{KD}(0, T')] \cdot (G \setminus [\text{DK}(t, T'), \text{DKD}(t, T')])'$ 
48: end function
49:
50: function VD0DF( $t, T, G$ )
51:   ► same as V0F(-) but for gradients
52:   return  $\text{DKD}(0, t) - [\text{DK}(0, T'), \text{DKD}(0, T')] \cdot (G \setminus [\text{DK}(t, T'), \text{DKD}(t, T')])'$ 
53: end function

```

```

1: _____
2: ► all following procedures use the same design parameter:
3:  $\tau \leftarrow 10$ 
4: _____
5: function K( $a, b$ )
6:   ► Wiener kernel integrated once in each argument
7:   return  $1/3 \odot \min(a + \tau, b + \tau).^3 + 0.5 \odot |a - b| \odot \min(a + \tau, b + \tau).^2$ 
8: end function
9:
10: function KD( $a, b$ )
11:   ► Wiener kernel integrated in first argument
12:   return  $0.5 \odot (a < b) \odot (a + \tau).^2 + (a \geq b) \odot ((a + \tau) \cdot (b + \tau) - 0.5 \odot (b + \tau).^2)$ 
13: end function
14:
15: function DK( $a, b$ )
16:   ► Wiener kernel integrated in second argument
17:   return  $0.5 \odot (a > b) \odot (b + \tau).^2 + (a \leq b) \odot ((a + \tau) \cdot (b + \tau) - 0.5 \odot (a + \tau).^2)$ 
18: end function
19:
20: function DKD( $a, b$ )
21:   ► Wiener kernel
22:   return  $\min(a + \tau, b + \tau)$ 
23: end function
24:
25: function DDK( $a, b$ )
26:   ► Wiener kernel integrated in second argument and 1x derived in first argument
27:   return  $(a \leq b) \odot (b - a)$ 
28: end function
29:
30: function DDKD( $a, b$ )
31:   ► Wiener kernel 1x derived in first argument
32:   return  $(a \leq b)$ 
33: end function

```

```

34: function DDDK( $a, b$ )
35:     ► Wiener kernel 2x derived in first argument and integrated in second argument
36:     return  $-(a \leq b)$ 
37: end function
    
```

```

1: function PROBWOLFE( $t, T, A, G$ )
2:     ► design parameters
3:      $c_1 \leftarrow 0.05$                                      ▷ constant for Armijo condition
4:      $c_2 \leftarrow 0.5$                                    ▷ constant for curvature condition
5:      $c_W \leftarrow 0.3$                                   ▷ threshold for Wolfe probability
6:
7:     ► mean and covariance values at start position ( $t = 0$ )
8:      $m_0 \leftarrow M(0, T, A)$ 
9:      $dm_0 \leftarrow D1M(0, T, A)$ 
10:     $V_0 \leftarrow V(0, T, G)$ 
11:     $Vd_0 \leftarrow VD(0, T, G)$ 
12:     $dVd_0 \leftarrow DVD(0, T, G)$ 
13:
14:    ► marginal mean and variance for Armijo condition
15:     $m_a \leftarrow m_0 - M(t, T, A) + c_1 \cdot t \cdot dm_0$ 
16:     $V_{aa} \leftarrow V_0 + (c_1 \cdot t)^2 \cdot dVd_0 + V(t) + 2 \cdot (c_1 \cdot t \cdot (Vd_0 - VD0F(t)) - V0F(t))$ 
17:
18:    ► marginal mean and variance for curvature condition
19:     $m_b \leftarrow D1M(t) - c_2 \cdot dm_0$ 
20:     $V_{bb} \leftarrow c_2^2 \cdot dVd_0 - 2 \cdot c_2 \cdot VD0DF(t) + DVD(t)$ 
21:
22:    ► covariance between conditions
23:     $V_{ab} \leftarrow -c_2 \cdot (Vd_0 + c_1 \cdot t \cdot dVd_0) + c_2 \cdot VD0F(t) + V0DF(t) + c_1 \cdot t \cdot VD0DF(t) - VD(t)$ 
24:
25:    ► extremely small variances → very certain (deterministic evaluation)
26:    if  $V_{aa} \leq 1^{-9}$  or  $V_{bb} \leq 1^{-9}$  then
27:         $p_{Wolfe} \leftarrow (m_a \geq 0) \cdot (m_b \geq 0)$ 
28:
29:        ► accept?
30:         $p_{acc} \leftarrow p_{Wolfe} > c_W$ 
31:        return  $p_{acc}$ 
32:    end if
33:
34:    ► zero or negative variances (maybe something went wrong?)
35:    if  $V_{aa} \leq 0$  or  $V_{bb} \leq 0$  then
36:        return 0
37:    end if
    
```

```

38:   ▶ noisy case (everything is alright)
39:   ▶ correlation
40:    $\rho \leftarrow V_{ab} / \sqrt{V_{aa} \cdot V_{bb}}$ 
41:
42:   ▶ lower and upper integral limits for Armijo condition
43:    $low_a \leftarrow -m_a / \sqrt{V_{aa}}$ 
44:    $up_a \leftarrow +\infty$ 
45:
46:   ▶ lower and upper integral limits for curvature condition
47:    $low_b \leftarrow -m_b / \sqrt{V_{bb}}$ 
48:    $up_b \leftarrow (2 \cdot c_2 \cdot (|dm_0| + 2 \cdot \sqrt{dVd_0}) - m_b) / \sqrt{V_{bb}}$ 
49:
50:   ▶ compute Wolfe probability
51:    $p_{Wolfe} \leftarrow \text{BVN}(low_a, up_a, low_b, up_b, \rho)$ 
52:
53:   ▶ accept?
54:    $p_{acc} \leftarrow p_{Wolfe} > c_W$ 
55:   return  $p_{acc}$ 
56:

```

The function $\text{BVN}(low_a, up_a, low_b, up_b, \rho)$ evaluates the 2D-integral

```

57:   
$$\int_{low_a}^{up_a} \int_{low_b}^{up_b} \mathcal{N} \left( \begin{bmatrix} a \\ b \end{bmatrix}; \begin{bmatrix} 0 \\ 0 \end{bmatrix}, \begin{bmatrix} 1 & \rho \\ \rho & 1 \end{bmatrix} \right) da db.$$


```

```

58:
59: end function

```

```

1: function GAUSSCDF( $z$ )
2:   ▶ Gauss cumulative density function
3:   return  $0.5 \odot (1 + \text{erf}(z / \sqrt{2}))$ 
4: end function
5:
6: function GAUSSPDF( $z$ )
7:   ▶ Gauss probability density function
8:   return  $\exp(-0.5 \odot z.^2) \odot \sqrt{2\pi}$ 
9: end function
10:
11: function EXPECTEDIMPROVEMENT( $m, s, \eta$ )
12:   ▶ Jones et al. (1998)
13:   return  $(\eta - m) \odot \text{GAUSSCDF}((\eta - m) \odot s) + s \odot \text{GAUSSPDF}((\eta - m) \odot s)$ 
14: end function

```

References

- R.J. Adler. *The Geometry of Random Fields*. Wiley, 1981.
- S.-I. Amari, H. Park, and K. Fukumizu. Adaptive method of realizing natural gradient learning for multilayer perceptrons. *Neural Computation*, 12(6):1399–1409, 2000.
- L. Armijo. Minimization of functions having Lipschitz continuous first partial derivatives. *Pacific Journal of Mathematics*, 16(1):1–3, 1966.
- L. Balles, J. Romero, and P. Hennig. Coupling Adaptive Batch Sizes with Learning Rates. *ArXiv e-prints*, December 2016.
- L. Bottou. Large-scale machine learning with stochastic gradient descent. In *Proceedings of the 19th Int. Conf. on Computational Statistics (COMPSTAT)*, pages 177–186. Springer, 2010.
- T. Broderick, N. Boyd, A. Wibisono, A.C. Wilson, and M.I. Jordan. Streaming variational Bayes. In *Advances in Neural Information Processing Systems (NIPS 26)*, pages 1727–1735, 2013.
- C.G. Broyden. A new double-rank minimization algorithm. *Notices of the AMS*, 16(4):670, 1969.
- Z. Drezner and G.O. Wesolowsky. On the computation of the bivariate normal integral. *Journal of Statistical Computation and Simulation*, 35(1-2):101–107, 1990.
- J. Duchi, E. Hazan, and Y. Singer. Adaptive subgradient methods for online learning and stochastic optimization. *Journal of Machine Learning Research*, 12:2121–2159, 2011.
- R. Fletcher. A new approach to variable metric algorithms. *The Computer Journal*, 13(3):317, 1970.
- R. Fletcher and C.M. Reeves. Function minimization by conjugate gradients. *The Computer Journal*, 7(2):149–154, 1964.
- A.P. George and W.B. Powell. Adaptive stepsizes for recursive estimation with applications in approximate dynamic programming. *Machine Learning*, 65(1):167–198, 2006.
- D. Goldfarb. A family of variable metric updates derived by variational means. *Math. Comp.*, 24(109):23–26, 1970.
- E. Hairer, S.P. Nørsett, and G. Wanner. *Solving Ordinary Differential Equations I – Nonstiff Problems*. Springer, 1987.
- P. Hennig. Fast Probabilistic Optimization from Noisy Gradients. In *30th International Conference on Machine Learning (ICML)*, 2013.
- J. Hensman, M. Rattray, and N.D. Lawrence. Fast variational inference in the conjugate exponential family. In *Advances in Neural Information Processing Systems (NIPS 25)*, pages 2888–2896, 2012.
- M.D. Hoffman, D.M. Blei, C. Wang, and J. Paisley. Stochastic variational inference. *Journal of Machine Learning Research*, 14(1):1303–1347, 2013.
- D.R. Jones, M. Schonlau, and W.J. Welch. Efficient global optimization of expensive black-box functions. *Journal of Global Optimization*, 13(4):455–492, 1998.
- Diederik P. Kingma and Jimmy Ba. Adam: A method for stochastic optimization. *CoRR*, abs/1412.6980, 2014. URL <http://arxiv.org/abs/1412.6980>.

- M. Mahsereci and P. Hennig. Probabilistic line searches for stochastic optimization. In *Advances in Neural Information Processing Systems 28*, pages 181–189, 2015.
- J. Martens. Deep learning via Hessian-free optimization. In *International Conference on Machine Learning (ICML)*, 2010.
- J. Nocedal and S.J. Wright. *Numerical Optimization*. Springer Verlag, 1999.
- A. Papoulis. *Probability, Random Variables, and Stochastic Processes*. McGraw-Hill, New York, 3rd ed. edition, 1991.
- R. Rajesh, W. Chong, D. Blei, and E. Xing. An adaptive learning rate for stochastic variational inference. In *30th International Conference on Machine Learning (ICML)*, pages 298–306, 2013.
- C.E. Rasmussen and C.K.I. Williams. *Gaussian Processes for Machine Learning*. MIT, 2006.
- H. Robbins and S. Monro. A stochastic approximation method. *The Annals of Mathematical Statistics*, 22(3):400–407, Sep. 1951.
- N.L. Roux and A.W. Fitzgibbon. A fast natural Newton method. In *27th International Conference on Machine Learning (ICML)*, pages 623–630, 2010.
- S. Särkkä. *Bayesian filtering and smoothing*. Cambridge University Press, 2013.
- T. Schaul, S. Zhang, and Y. LeCun. No more pesky learning rates. In *30th International Conference on Machine Learning (ICML-13)*, pages 343–351, 2013.
- N.N. Schraudolph. Local gain adaptation in stochastic gradient descent. In *Ninth International Conference on Artificial Neural Networks (ICANN) 99*, volume 2, pages 569–574, 1999.
- D.F. Shanno. Conditioning of quasi-Newton methods for function minimization. *Math. Comp.*, 24(111):647–656, 1970.
- Ilya Sutskever, James Martens, George Dahl, and Geoffrey Hinton. On the importance of initialization and momentum in deep learning. In *Proceedings of the 30th International Conference on Machine Learning (ICML-13)*, volume 28. JMLR Workshop and Conference Proceedings, 2013.
- G. Wahba. *Spline models for observational data*. Number 59 in CBMS-NSF Regional Conferences series in applied mathematics. SIAM, 1990.
- P. Wolfe. Convergence conditions for ascent methods. *SIAM Review*, pages 226–235, 1969.
- T. Zhang. Solving large scale linear prediction problems using stochastic gradient descent algorithms. In *Twenty-first International Conference on Machine Learning (ICML 2004)*, 2004.